EFFECTS OF REYNOLDS NUMBER ON SWEPT-WING-BODY CONFIGURATIONS WITH HIGH LIFT DEVICES AT TRANSONIC SPEEDS

E. Atraghji*
H. Sorensen**

* National Aeronautical Establishment (NAE), Canada
** The Aeronautical Research Institute (FFA), Sweden

ABSTRACT

Reynolds number effects in the range $1x10^6 < Re < 5x10^6$ and $0.5 < M < 0.95$ were investigated experimentally on swept-wing-body configurations with various degrees of leading edge droop. For the models with zero droop the effects of Reynolds number are found to be quite large at Mach 0.5, especially, on the axial force, the lift dependent drag and buffet onset. These effects are progressive in the Reynolds number range investigated and show no asymptotic tendency towards the upper part of the range. The observed effects decrease with rising Mach number. However, at supercritical Mach numbers, the pitching moment at small angles of attack shows considerable Reynolds number dependency.

Similar effects are observed on the configurations having leading edge droop but these effects are smaller than those for the zero droop cases.

PRINCIPAL NOTATION

α	angle of attack in degrees
M	free stream Mach number
Re	Reynolds number based on mean aerodynamic chord
δe	leading edge droop angle in degrees
C_N	normal force coefficient
C_m	pitching moment coefficient
C_X	axial force coefficient
Λ	sweep angle of quarter chord line in degrees
m_{RMS}	RMS value of the wing root bending moment

Subscripts

i,m,o = inner, middle and outer respectively

1. Introduction

There is a growing interest in developing aircraft capable of performing tight manoeuvres in the transonic Mach number regime, a regime that has hitherto been speedily avoided. When attempting tight manoeuvres, a means for generating high lift without incurring a severe drag penalty and/or buffeting is a desirable prerequisite. Another equally desirable requirement is to reduce the complexity of the high lift devices if these are to be used.

In an effort to explore the possibility in this field on potential aircraft configurations, a joint experimental investigation was undertaken by the FFA, Sweden and the NAE, Canada. The investigation was carried out in the FFA's 1mx1m S4 wind tunnel and the NAE's 1.5mx1.5m trisonic blowdown wind tunnel. The results from both wind tunnels are discussed below.

It is well known that rearward swept wings have a tendency to develop undesirable spanwise flow towards the tips, see Figure 1, which results in a degradation of the two dimensional aerofoil characteristics[1]. The reason being that the effective profile of the aerofoil changes due to the thickening of the boundary layer in these regions.

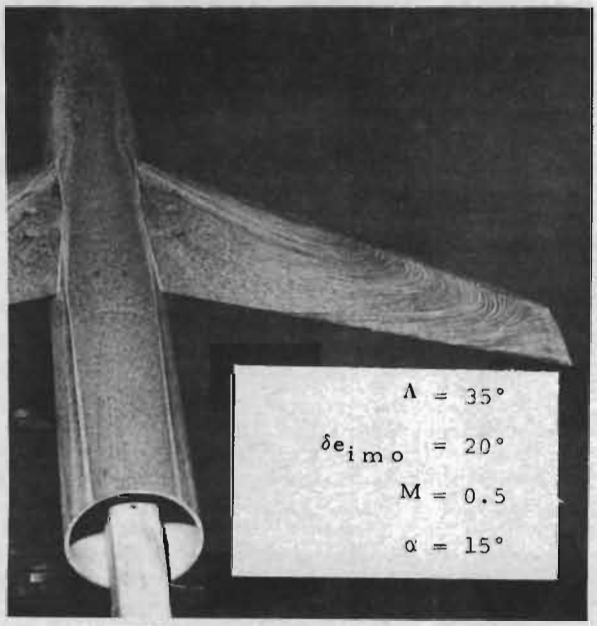

FIGURE 1 - FLOW VISUALIZATION TEST CONDUCTED AT FFA

In such cases a premature trailing edge stall at the tips could be caused giving rise to an early and unwanted pitch-up condition. This problem becomes even more acute when high lift devices are

incorporated to improve the maximum achievable C_L required for high speed manoeuvres. Since a high price is usually paid for the use of such devices at high speeds, namely, added structural weight and complexities to the control system, their effectiveness at representative flight Reynolds number must be assessed before their addition could be contemplated.

During earlier tests conducted at FFA[2], on a model having a wing with different sweep - back angles, it was noted that a leading edge droop gave increased normal force by delaying the leading edge separation to a higher angle of attack. Since the effects of separation and its suppression by drooping the leading edge have a tendency to be exaggerated at low Reynolds numbers, it was suspected that the apparent improvement in normal force caused by drooping the leading edge at the low Reynolds number achieved at FFA may not hold at higher Reynolds number. Therefore, a test at higher Reynolds number was conducted at the NAE in order to evaluate more appropriately the benefits of leading edge droop at representative near full-scale Reynolds number. The various features of this model chosen for investigation were based on further research work in the field as reported for example in References 3 and 4.

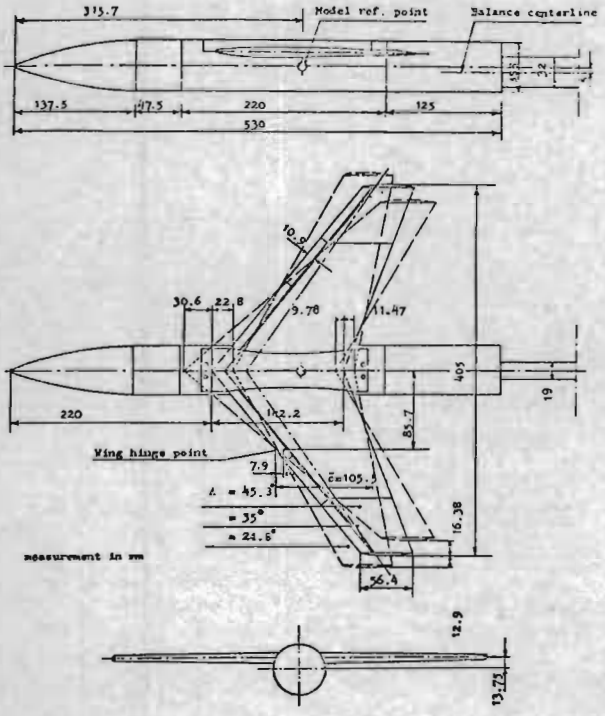

FIGURE 2 - DETAILS OF TEST MODEL PT1

The choice of sweep-back angles was based on a desire to study the changes in the character of the flow and in particular to the type of stall that might be encountered with a change in the sweep-back angle. In Reference 5 a description is provided of how it is possible for a leading edge type stall to change to a trailing edge stall at the tip region with increasing sweep-back angle. As we explained earlier, the reason for this change in stalling characteristics is the thickening of the boundary layer towards the tip as a result of the spanwise outboard flow on the upper surface of the wing. In an effort to reduce this tipwise flow, upwardly curved wing tips were proposed for testing by the NAE. Moreover, from the FFA tests [2] it was noted that with the uniform droop along the leading edge the separation tended to start at the wing tips. In attempting to delay such a separation a variable droop along the span of the 35° sweep angle configuration was also investigated. The variable droop is such that it increases towards the tips.

In the evaluation of the characteristics of the various configurations the onset of buffet plays an important role. In the present investigation strain gauges were used to measure the wing root bending moment as an indication of buffet onset. In the FFA's S4 wind tunnel good correlation was obtained between the root mean square (RMS) signal from this gauge and the separation drag rise as shown in the axial force curve. In the NAE wind tunnel facility the RMS method of measuring buffet onset was not successful due to the high ambient noise level during the run and a natural frequency of the balance model system close to one of the dominant 'noise' frequencies. For the tests performed at the NAE the separation drag rise was used as indication of buffet onset. The results obtained using this method correlate well with buffet onset measurements obtained from the test at FFA. The usefulness of this method has been verified by others as for example Reference 6.

2. Model Description

Details of the complete model configuration used in the investigation are given in Figure 2. The wing can be installed at quarter-chord sweep-back angles of 25°, 35° and 45°. The variation in sweep angle is obtained by changing the wing bracket.

At the 35° sweep angle the wing has a span of 405 mm, an aspect ratio of 4 and a taper ratio of 0.4. The wing has a NACA 64A010 airfoil section normal to the quarter-chord line. The wing tips

can be changed between straight and upwardly curved tips, see Figure 2B. The droop angle of the three leading edge segments can be changed by changing the mounting brackets.

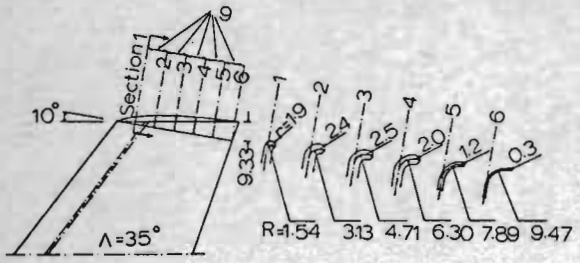

FIGURE 2B - NAE WING TIPS

The centre body or fuselage, consists of a circular cylinder with a tangent ogive pointed nose section.

With respect to high Reynolds number tests the finish of the model was made as smooth as practicable, say 0.2 micron, apart from joints which were filled with wax. Some tests with artificial boundary layer transition trips were conducted at FFA. Their location and type are given in Figure 2C. However, the major part of the tests at FFA and all tests at NAE were made with clean models (no trips).

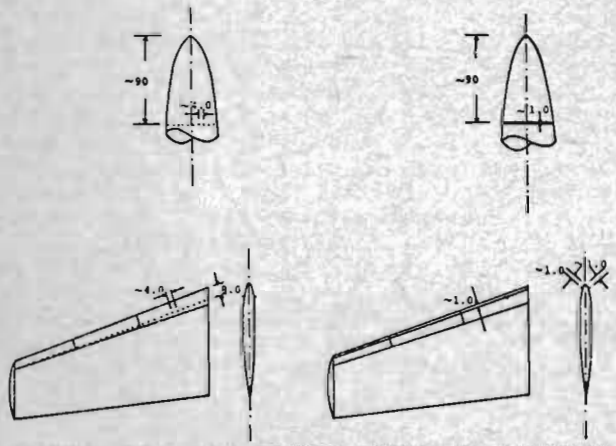

FIGURE 2C - ARTIFICIAL MEANS OF BOUNDARY LAYER TRIPS USED - STEEL BALLS (L) AND SAND STRIP (R)

3. Test Programme

The test programme is specified in tables I, II and III. The order of testing followed the order shown in these tables.

TABLE I
6-COMPONENT BALANCE TEST IN THE FFA'S S4 WIND TUNNEL

Λ 1/4C	$\delta e_{i,m,o}$	M .5	.8	.9	.95	$Rex10^{-6}$
25	0, 0 , 0	x	x	x	x	1.0-1.5
35	"	x	x	x	x	1.1-1.6
"	20, 20 ,20	x	x	x		"
"	10,15 ,20	x	x	x		"
"	5,7.5,10	x	x	x		"
"	0, 0 , 0	x	x	x		" *
45	"	x	x	x	x	1.3-1.9

* test performed with transition trips steel balls and grain of sand

TABLE II
BUFFETING MEASUREMENTS IN THE FFA'S S4 WIND TUNNEL

1/4C Λ	$\delta e_{i,m,o}$	M	$Rex10^{-6}$
35	0, 0 , 0	0.5	1.1
"	20,20 ,20	"	"
"	0, 0 , 0	0.9	1.6
"	20,20 ,20	"	"

TABLE III
6-COMPONENT BALANCE TEST IN THE NAE'S 1.5 METRE SQUARE WIND TUNNEL

Λ 1/4C	$\delta e_{i,m,o}$	M .5	.8	.9	.95	$Rex10^{-6}$
35	0, 0 , 0	x	x	x	x	2,3,4,5
"	"	x				1.5
"	"	x	x	x	x	2,4*
"	20, 20 ,20	x	x	x		2,3,4,5
"	10, 15 ,20	x				2,3,4,5
"	5,7.5,10		x	x		2,3,4,5
45	0, 0 , 0	x	x	x	x	2,3,4,5
25	"	x	x	x	x	2,3,4,5

* test performed with NAE tips.

4. Repeatability Considerations

The level of certainty of the results was established by repeatability checks. These checks were conducted on the basic, 35° sweep angle configuration. Two runs A and B were performed in the FFA's wind tunnel and three runs A, B and C were performed in the NAE's tunnel. The A and B runs were conducted on two different days but without disturbing the model while the C run was conducted after the model had been disassembled and reassembled. In each comparable case, exactly the same tunnel geometry was set up.

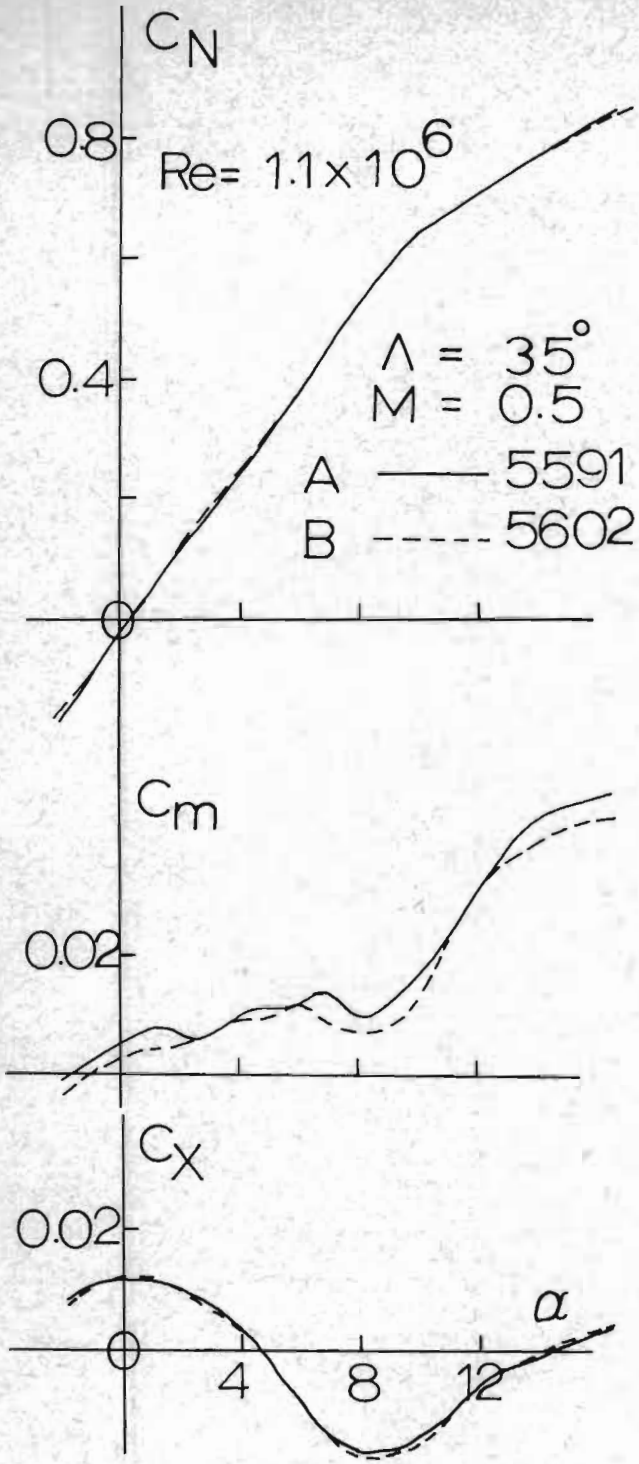

FIGURE 3A REPEATABILITY CHECKS (FFA)

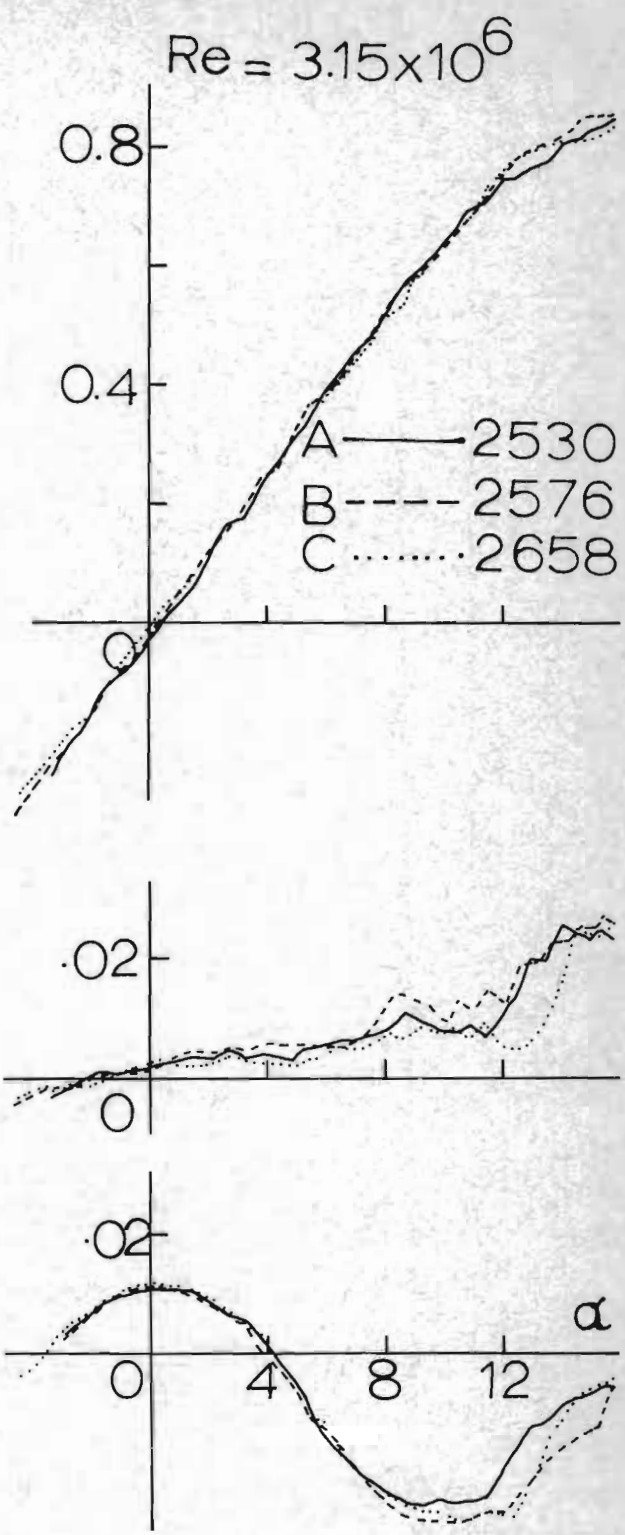

FIGURE 3B - REPEATABILITY CHECKS (NAE)

In Figure 3 comparisons of plots of C_N, C_m and C_X versus α are presented. It is clear from this figure that the agreement between the results of the repeatability tests is rather good for small and moderate angles of attack, but, noticeable deviations are observed at the higher angles of attack where flow separation has occured, i.e. subsequent to the departure of the axial force C_X from the parabolic variation with α. The angle of attack at which this departure takes place is estimated at about 7°. The reason for the discrepancies might likely be attributed to a roughening of the model surface through usage, especially in the region of the leading edge where it gets bombarded by small particles that blow down the tunnel from time to time. The effect of roughness, shown in Figure 4, will be further discussed in section 5.3 below.

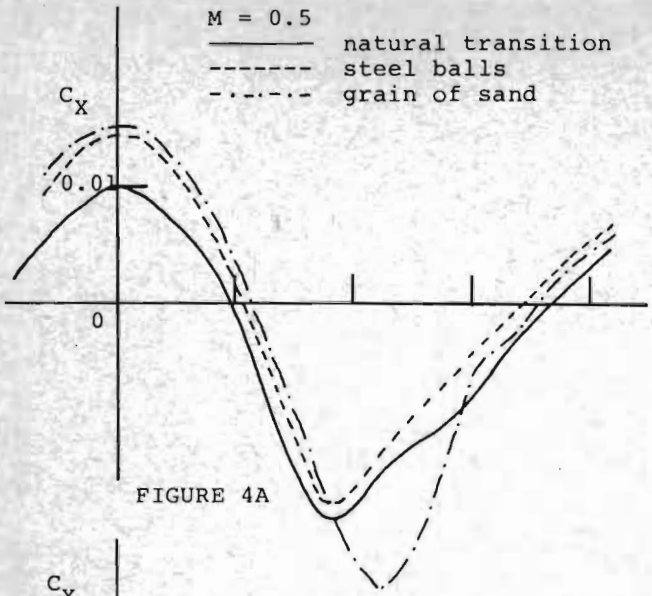

FIGURE 4A

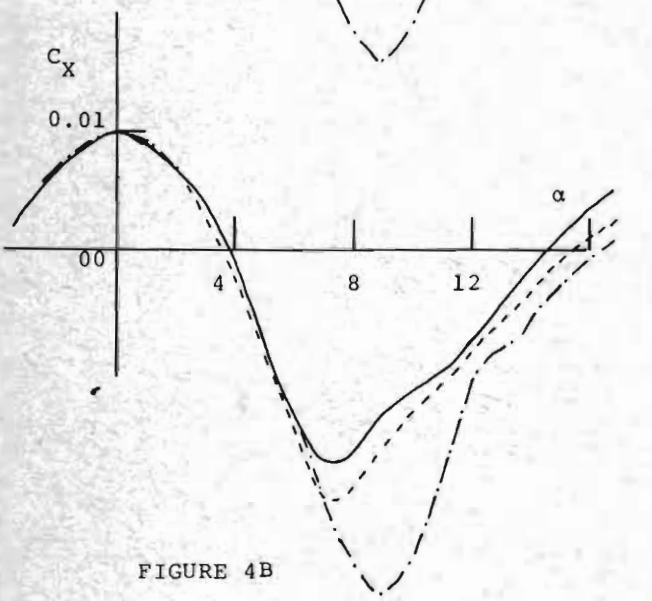

FIGURE 4B

FIGURE 4 - COMPARISONS OF C_X VERSUS α AT M = 0.5 BETWEEN RUNS WITH NATURAL AND ARTIFICIAL TRANSITION

5. Reynolds Number Effects

We proceed now to discuss the influence of the Reynolds number on the aerodynamic coefficients of normal force, C_N, pitching moment, C_m, and axial force, C_X.

In general it was found that the Reynolds number effects are progressive. It is therefore deemed sufficient in this presentation to compare only the results from the low Reynolds number tests at FFA and NAE with the results at the highest Reynolds number obtained at NAE. Any intermediate Reynolds number results may be found in References 7 and 8.

5.1 Reynolds Number Effects ON C_N

In Figure 5 the effects of Reynolds number on C_N are shown for the various test Mach numbers conducted.

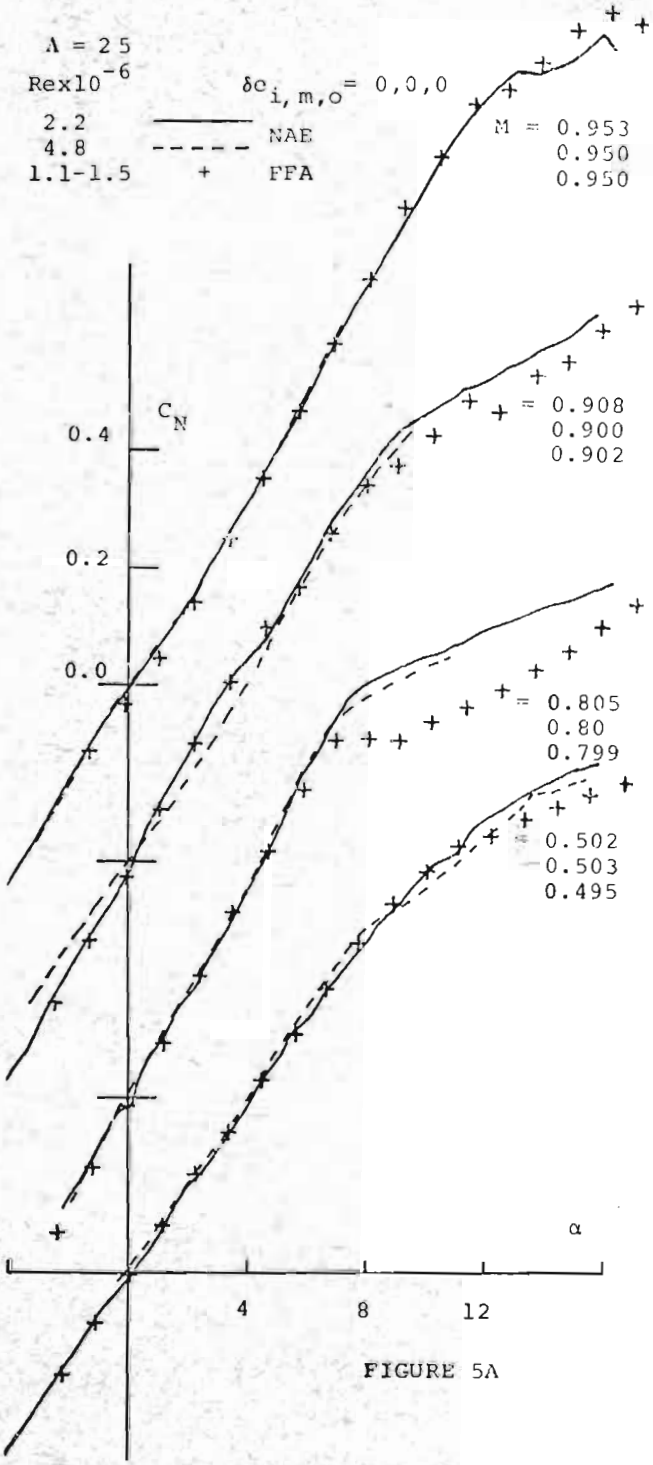

FIGURE 5A

FIGURE 5 - COMPARISONS OF C_N VERSUS α AT THREE REYNOLDS NUMBERS FOR THE VARIOUS MACH NUMBERS AND SWEEP ANGLES INVESTIGATED

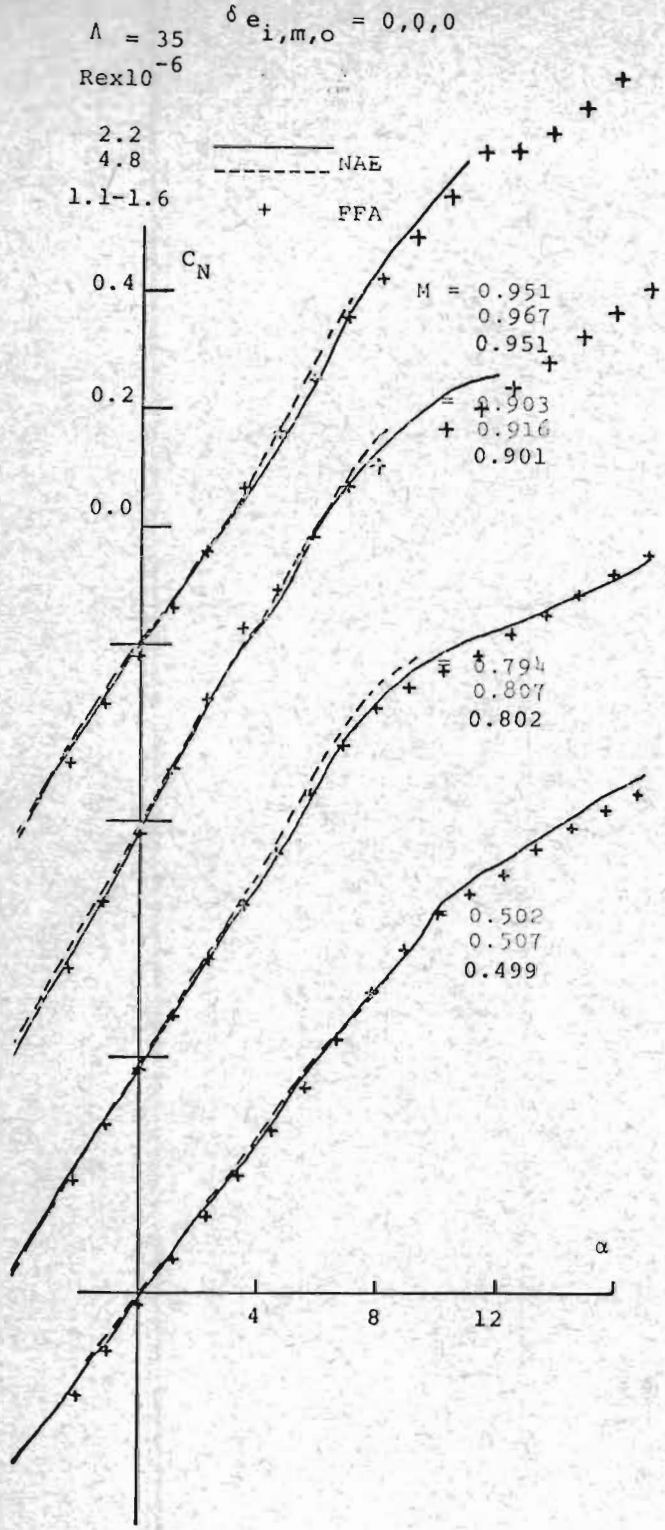

FIGURE 5B

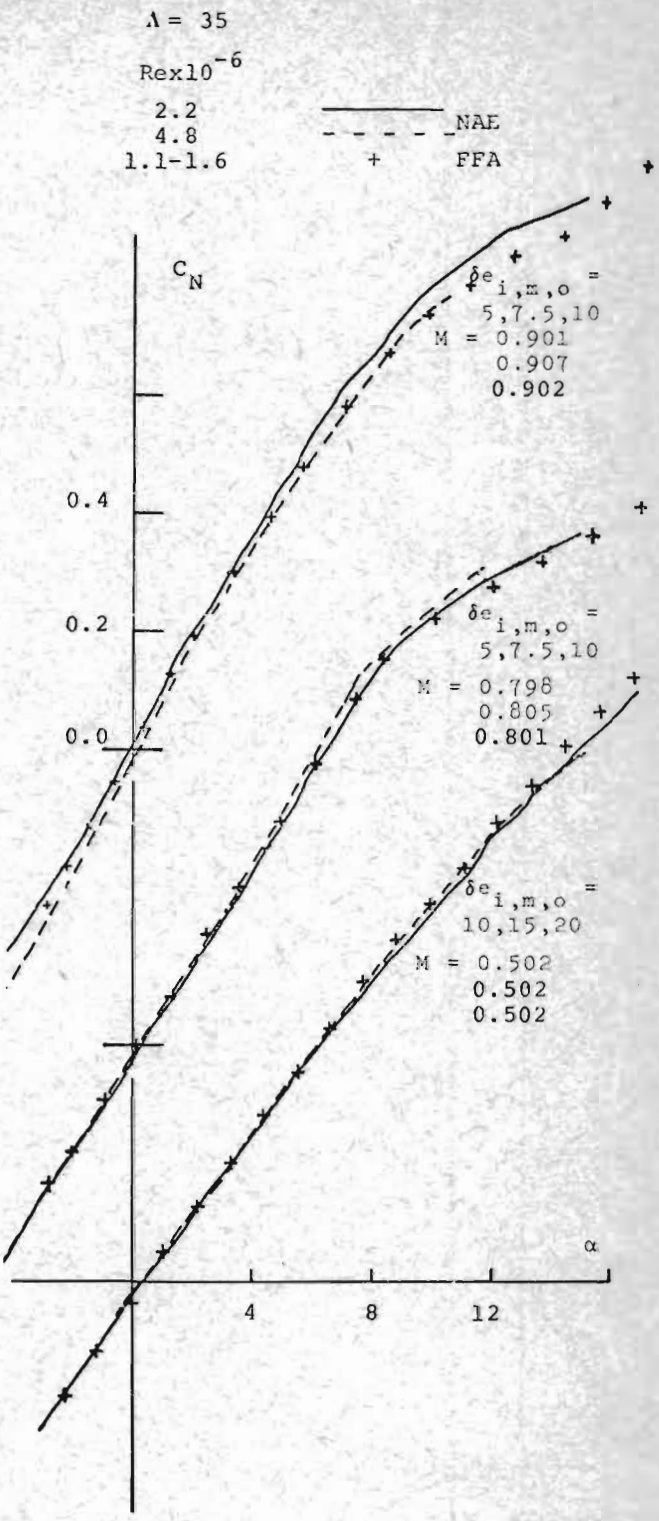

FIGURE 5C

The largest Reynolds number effects on C_N are observed at large angles of attack in the form of an increase in C_N with increasing Reynolds number. This is encountered, particularly, on the 25° sweep angle configuration. This effect

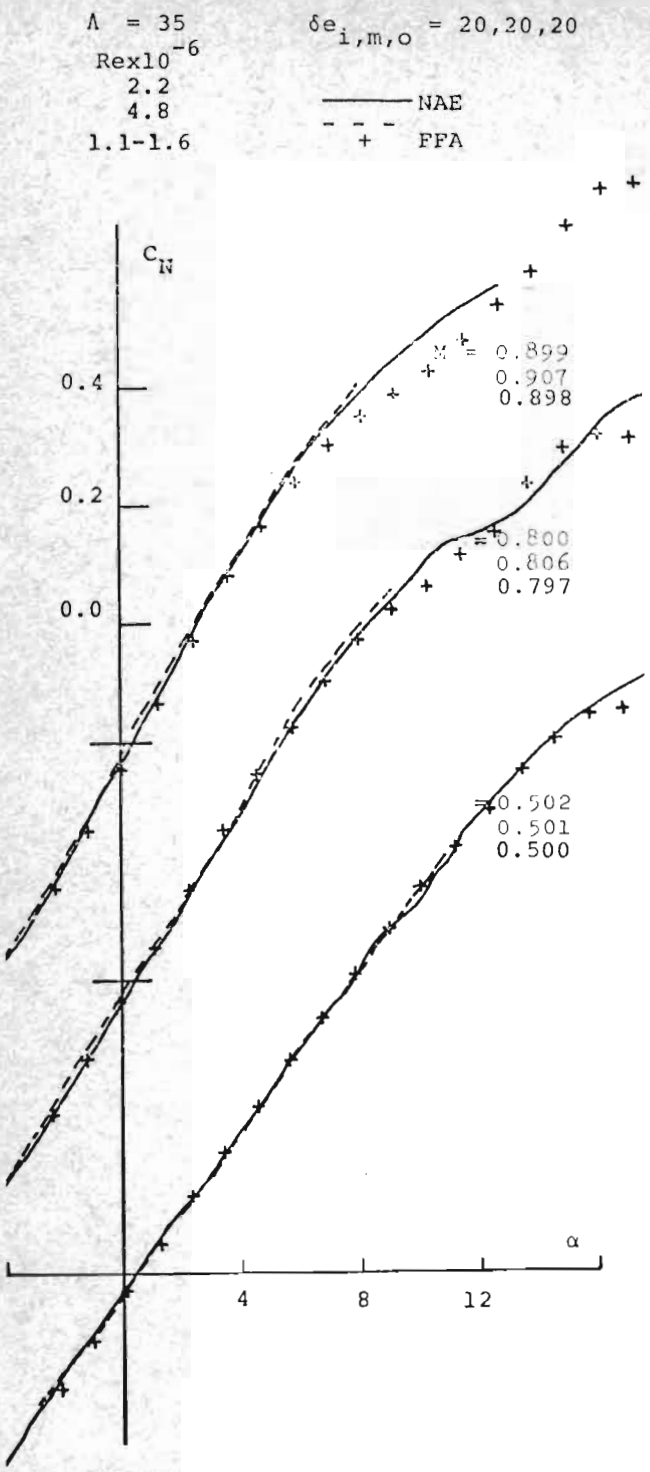

FIGURE 5D

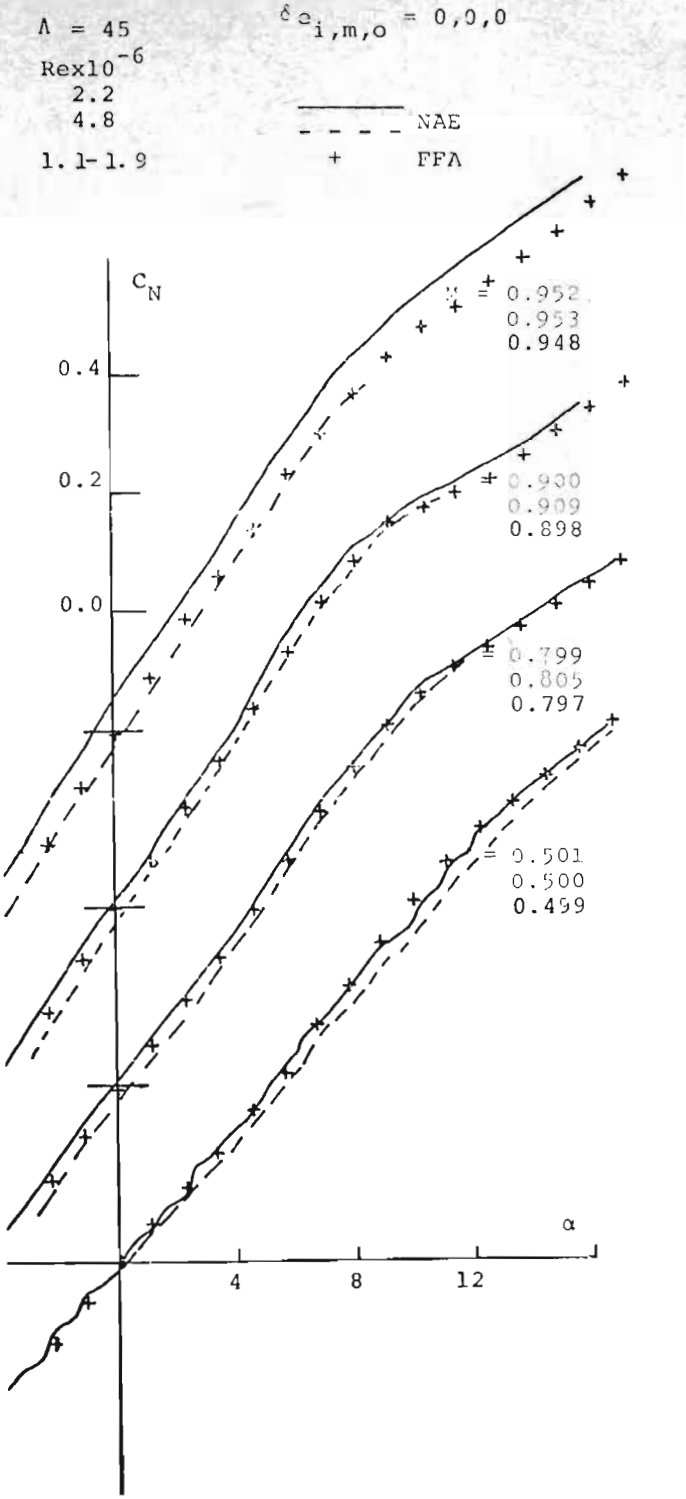

FIGURE 5E

decreases at 35° sweep angle. At 45° sweep angle there appears to be a uniform increment in C_N for the lowest Reynolds number tested at the NAE compared with that at the highest Reynolds number. This increment in C_N is largest at the highest test Mach number M = 0.95. No plausible explanation for this anomaly can be offered at present.

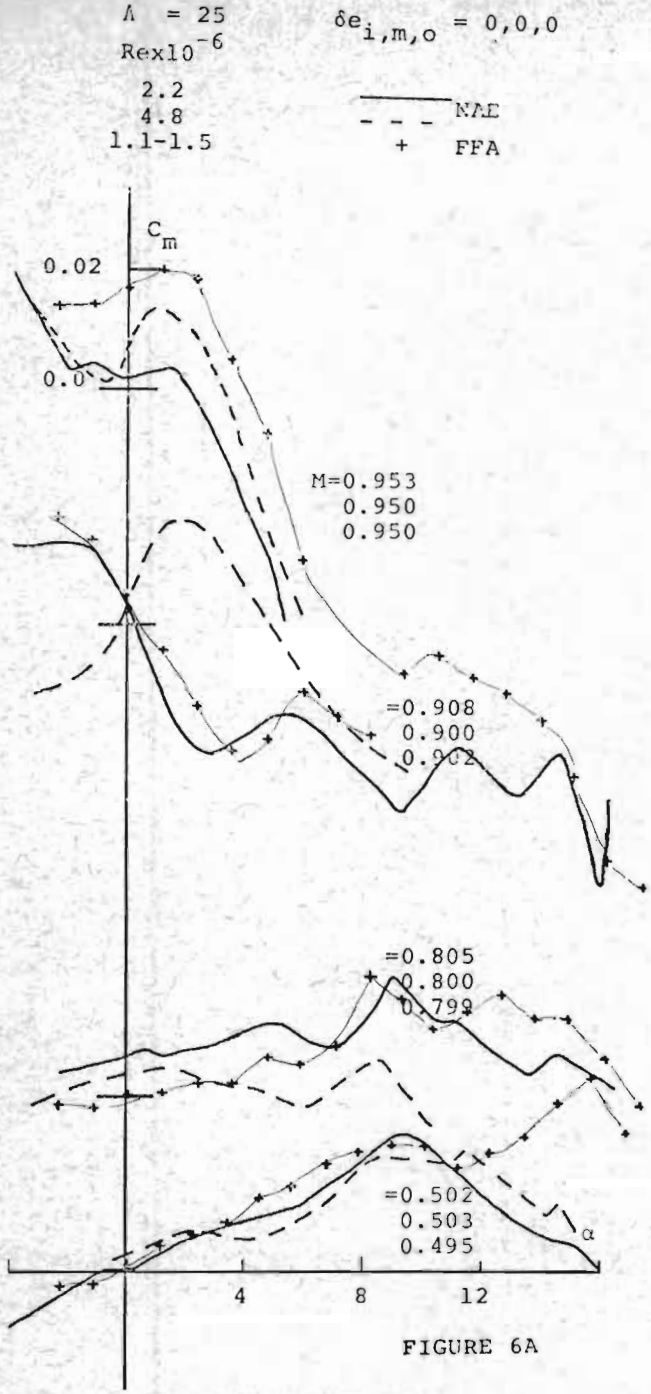

FIGURE 6A

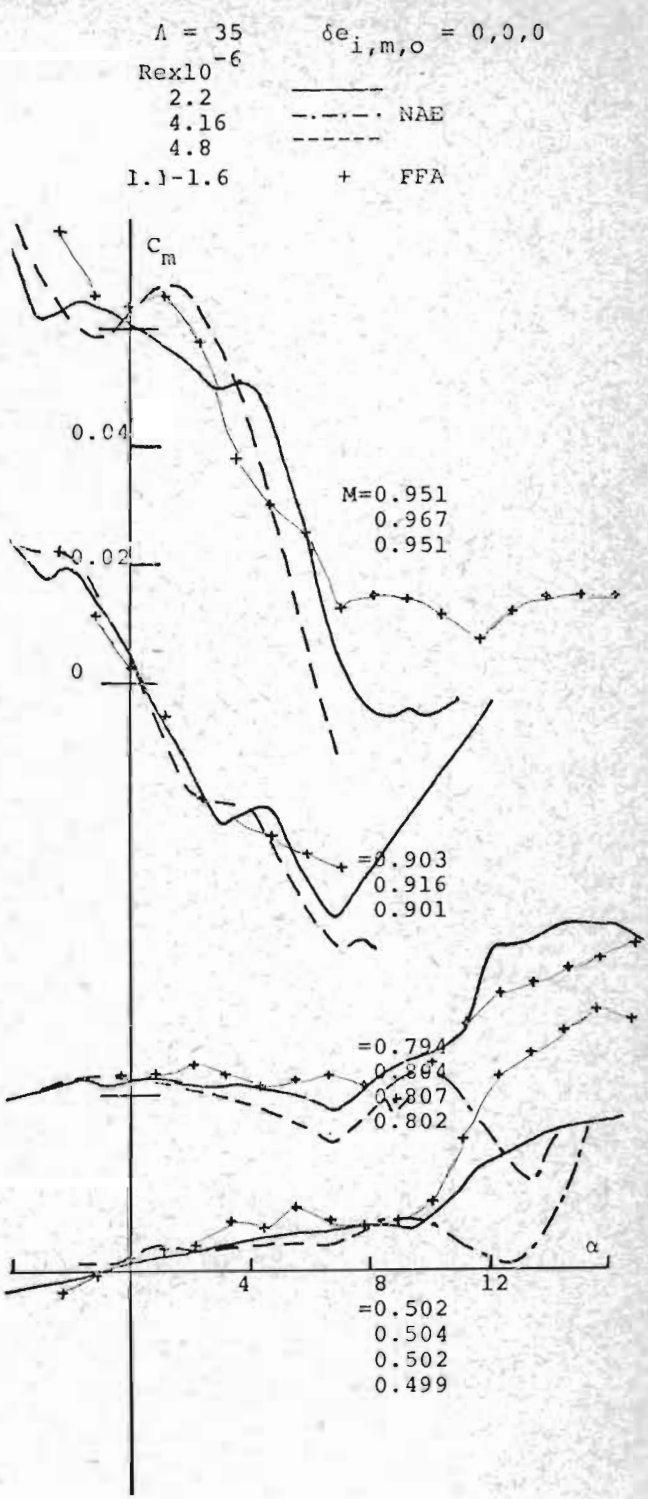

FIGURE 6B

FIGURE 6 - COMPARISONS OF C_m VERSUS α AT THREE REYNOLDS NUMBERS FOR THE VARIOUS MACH NUMBERS AND SWEEP ANGLES INVESTIGATED

5.2 Reynolds Number Effects on C_m

Comparisons of plots of C_m versus α are shown in Figure 6. The Reynolds number effects on pitching moment, seen as a decrease in the magnitude of the pitching moment, are most pronounced at the sweep angles $\Lambda = 25°$ and $35°$. For the lower Mach numbers M = 0.5 and 0.8 the effects are found especially at large angles of attack. For supercritical Mach numbers (M = 0.9 and 0.95 for $\Lambda = 25°$ and M = 0.95 for $\Lambda = 35°$) the character of the pitching moment curve changes noticeably with Reynolds number at small angles of attack resulting in reversed sign for the slope of the C_m versus α curve.

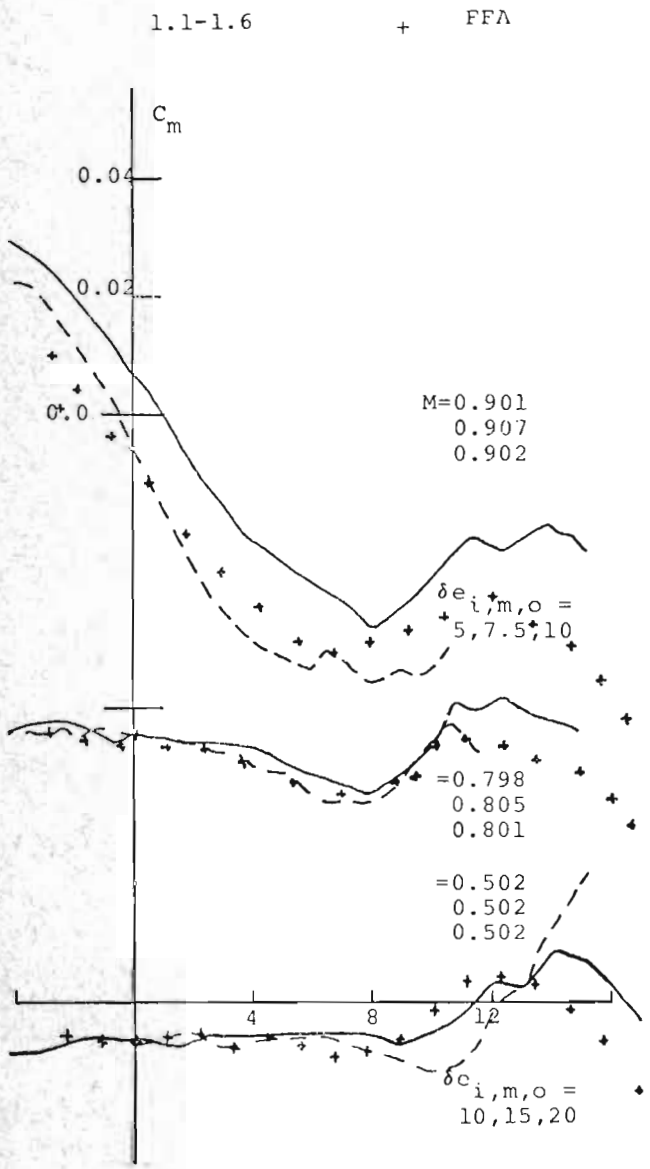

FIGURE 6C

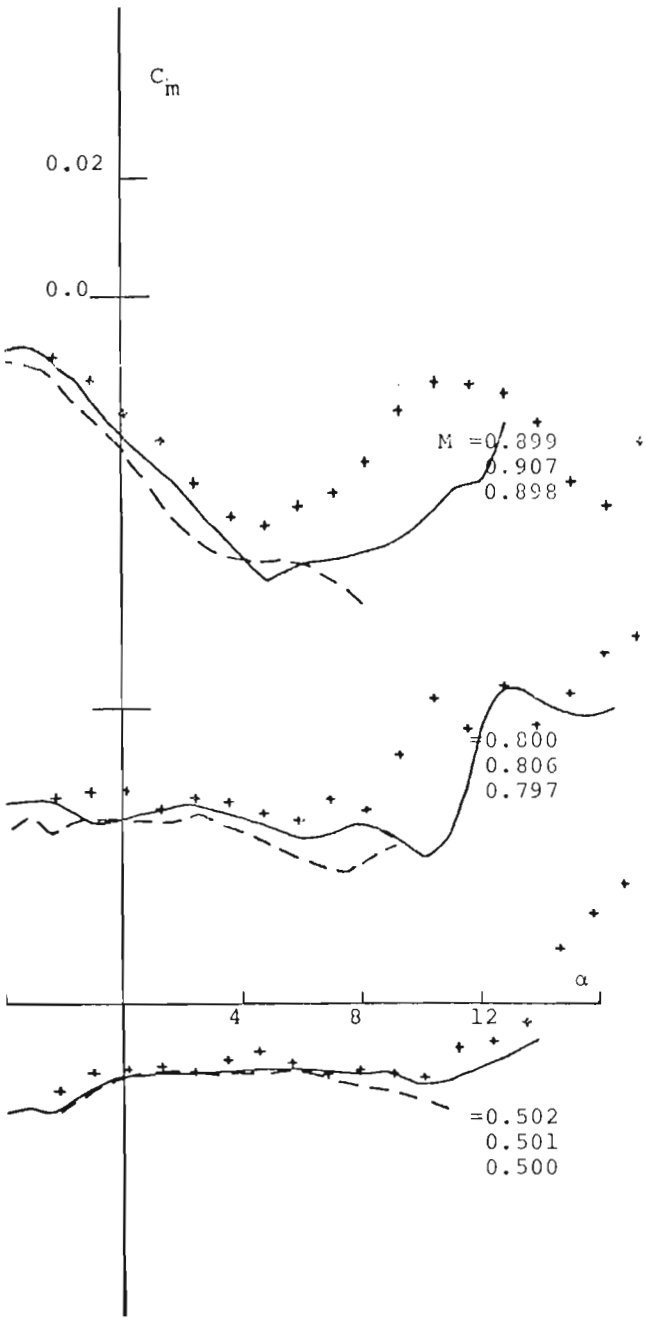

FIGURE 6D

It is not known whether such a reversal would have occurred on the drooped leading edge configurations with the 35° sweep at M=0.95, because the maximum Mach number at which these configurations were investigated was M = 0.9.

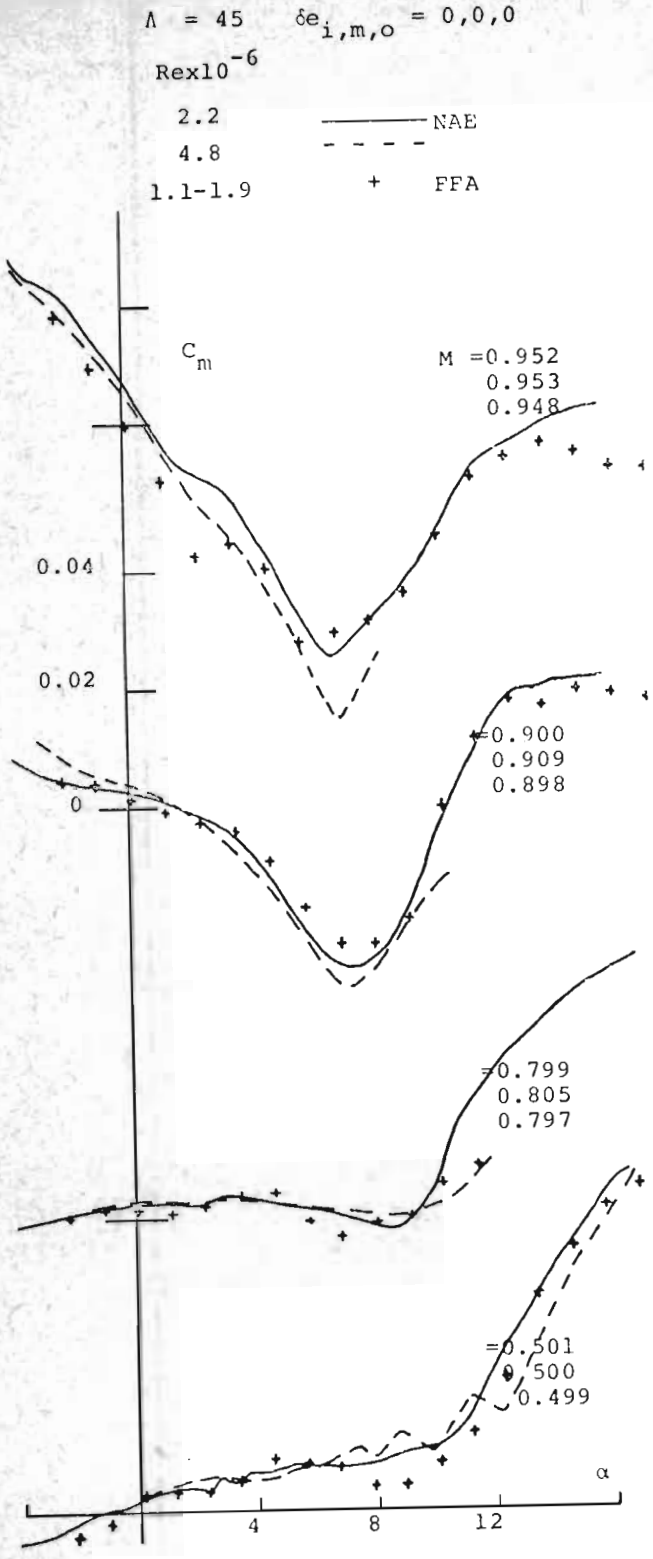

FIGURE 6E

The Reynolds number effects on the pitching moment characteristics of the 45° swept wing are small but increase with increasing angle of attack and Mach number. The pitch-up angle of attack is unaffected and no reversed slope at low angles of attack is observed at this sweep angle.

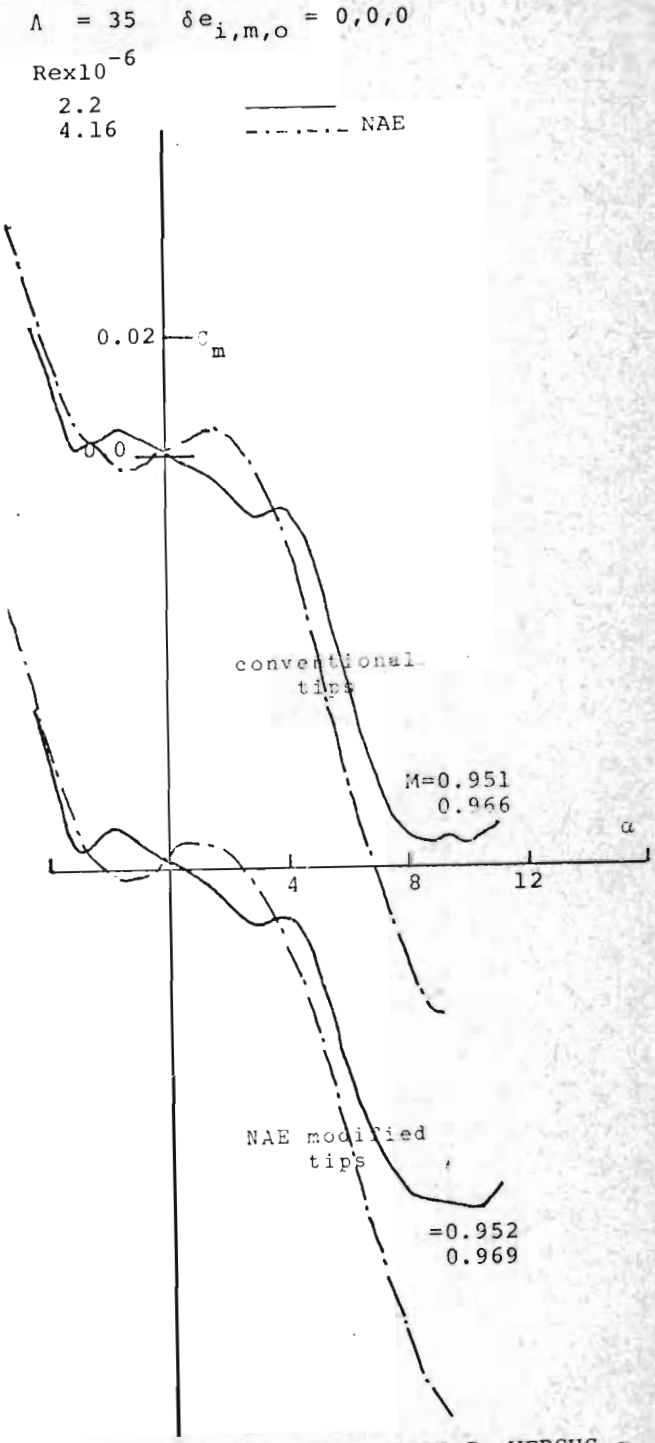

FIGURE 7 - COMPARISONS OF C_m VERSUS α BETWEEN REYNOLDS NUMBER 2.2×10^6 AND 4.16×10^6 USING THE CONVENTIONAL AND NAE MODIFIED WING TIPS

In Figure 7 the pitching moment curves for the two types of tips tested are shown at M = 0.95. It is seen that the modified upwardly curved tips display the same type of Reynolds number effects as the straight wing tips.

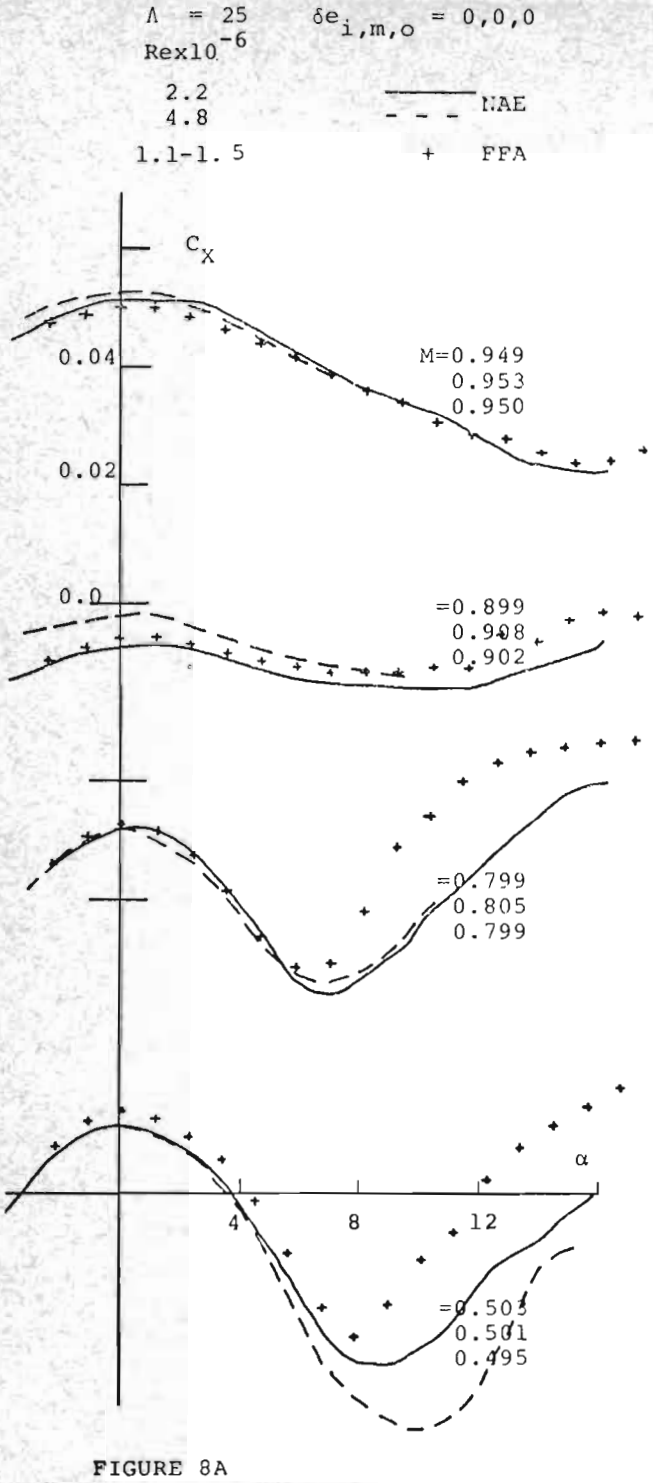

FIGURE 8A

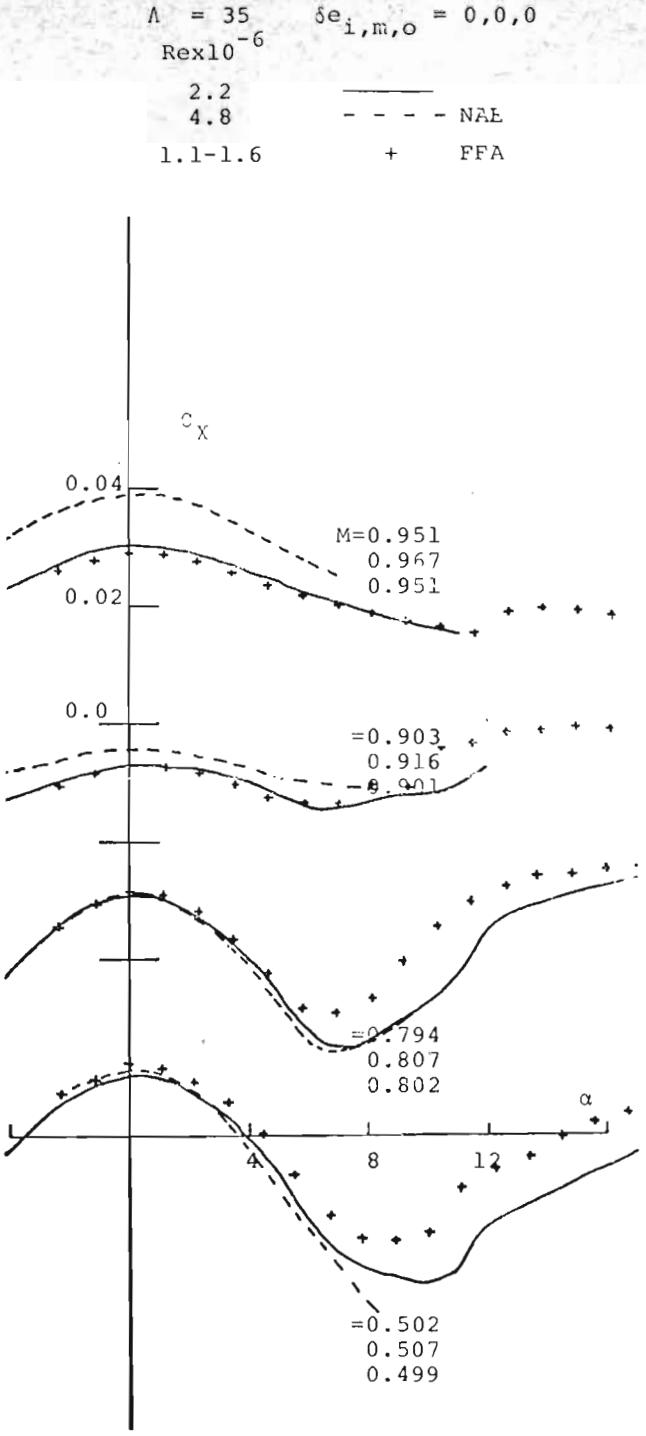

FIGURE 8B

FIGURE 8 - COMPARISONS OF C_X VERSUS α AT THREE REYNOLDS NUMBERS FOR THE VARIOUS MACH NUMBER AND SWEEP ANGLES INVESTIGATED

5.3 Reynolds Number Effects on C_X and C_D

In Figure 8 comparisons are shown between the axial force coefficient, C_X, at the two extreme Reynolds numbers investigated. From this figure we readily see that for the basic configurations investigated at M = 0.5 the effect on C_X of an increase in the Reynolds number is quite large at high angles of attack. These effects seem to be progressive in the whole range of Reynolds number showing no tendency to vanish in the upper part. However, with

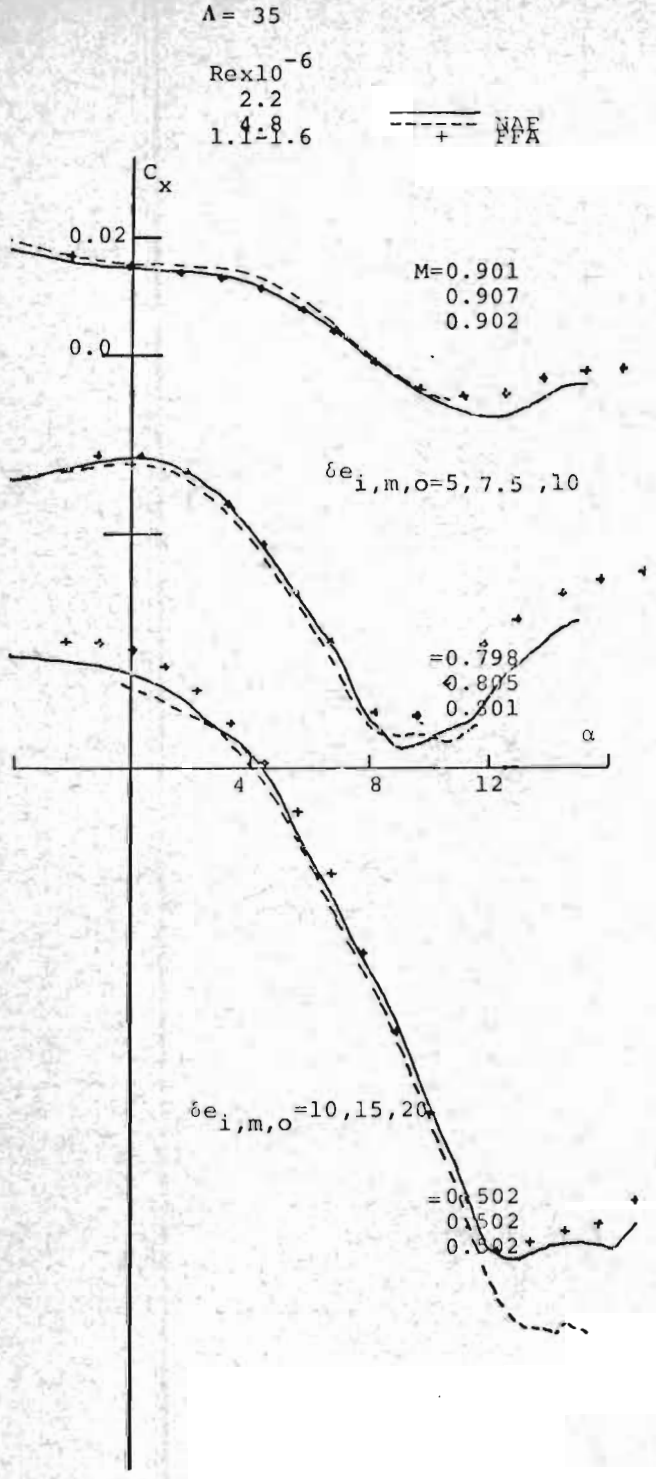

FIGURE 8C

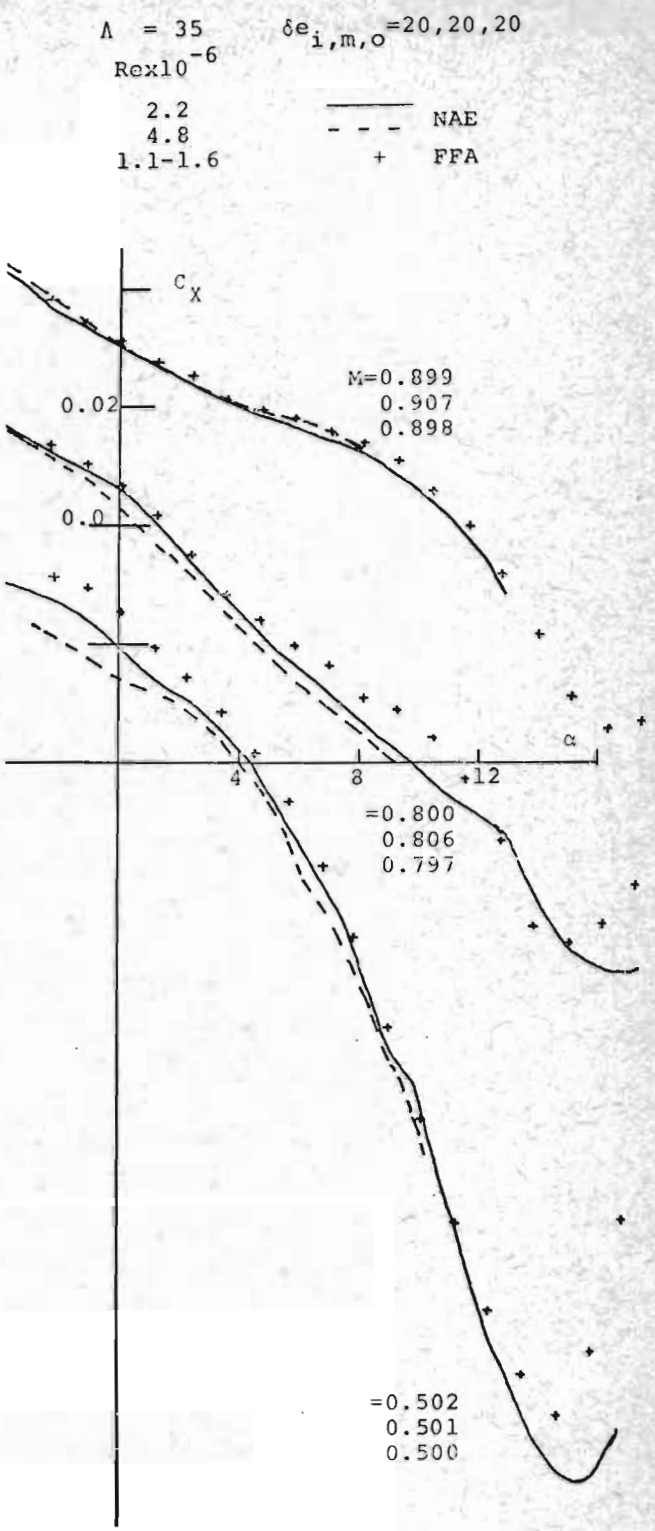

FIGURE 8D

increasing Mach number these Reynolds number effects decrease. The usual expected trend, namely, that an increase in the Reynolds number results in a delayed separation, or a decrease in the axial force coefficient at high angles of attack, has been found to hold in the Reynolds number range investigated.

The models with leading edge droop show similar Reynolds number effects but they are smaller than those encountered by the basic, zero leading edge droop, configuration.

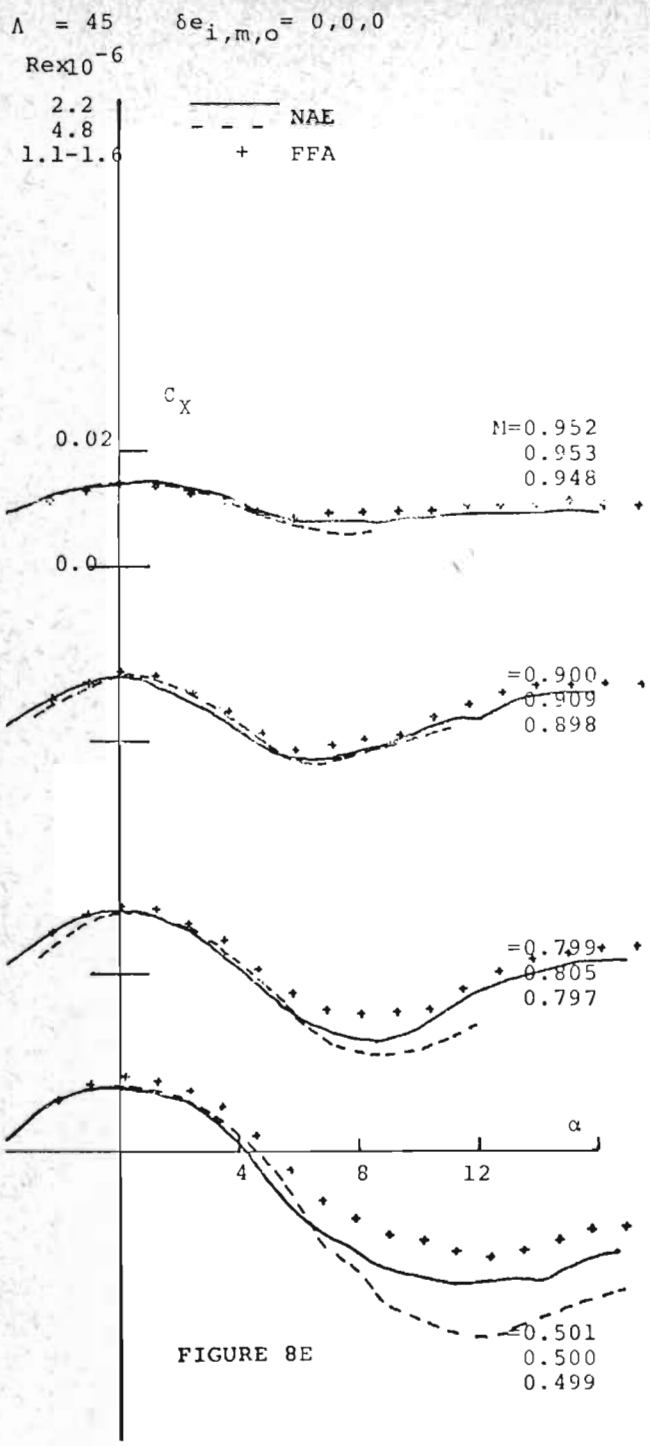

FIGURE 8E

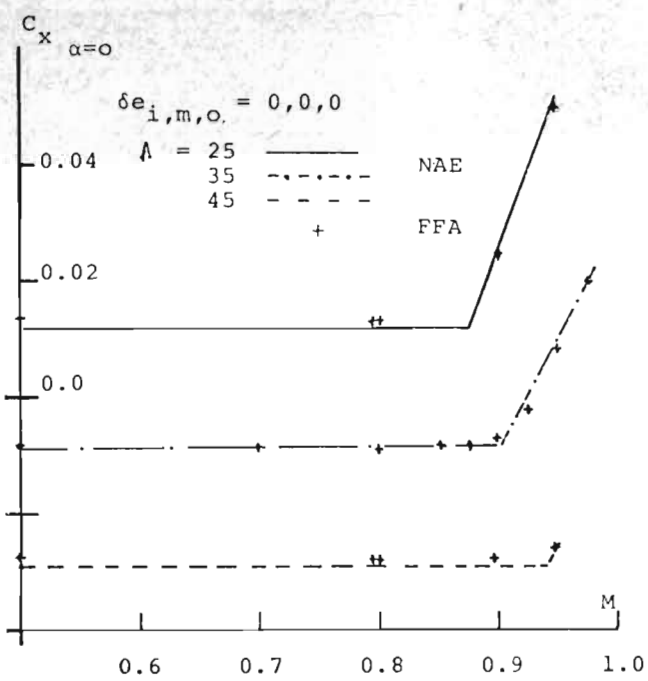

FIGURE 8F $C_X\big|_{\alpha=o}$ VERSUS α COLLATION OF DATA FOR THE HIGHEST AND LOWEST REYNOLDS NUMBERS TESTED

It should be noted that the positive shifts in the axial force observed at M = 0.9 and 0.95, see Figures 8A and 8B, are attributed to the small differences noted in the Mach number, from run to run, where this Mach number happens to be above the critical, or drag rise, Mach number. See insert of $C_X|_{\alpha\cong 0}$ versus M in Figure 8F. These shifts should not be confused then with Reynolds number effects but rather taken to be Mach number effects.

In Figure 4A, discussed previously, the axial force coefficient, C_X, is shown for the clean wing, and, for the wing equipped with two different means of artificial transition. It is noted in this figure that there is an increase in the value of C_X at $\alpha = 0$ when artificial transition is employed. This increase in axial force is due to earlier transition and to additional drag on roughness extending beyond the local boundary layer thickness which is commonly called protruberance drag. In Figure 4B, where the excess drag has been compensated for by a curve shift, the picture obtained is not too dissimilar from what we observe in Figure 8. A conclusion of this seems to be that test results for a model with transition trips in some way correspond to results for a clean model at a higher Reynolds number for the same Mach number. It is a well known fact though that it is still impossible to use this technique in a systematic way. Further, the repeatability comparisons shown in Figure 3B emphasize the need for a much better control at high Reynolds number testing on the parameters that are likely to influence the measurements, namely, surface finish and possibly tunnel turbulence level. For the sake of informing the reader, therefore, as to how 'aged' the surface of the model was at any particular comparison, the reader should note that testing was always made from low to high Reynolds numbers and low to high Mach numbers in the order shown in Tables I, II and III.

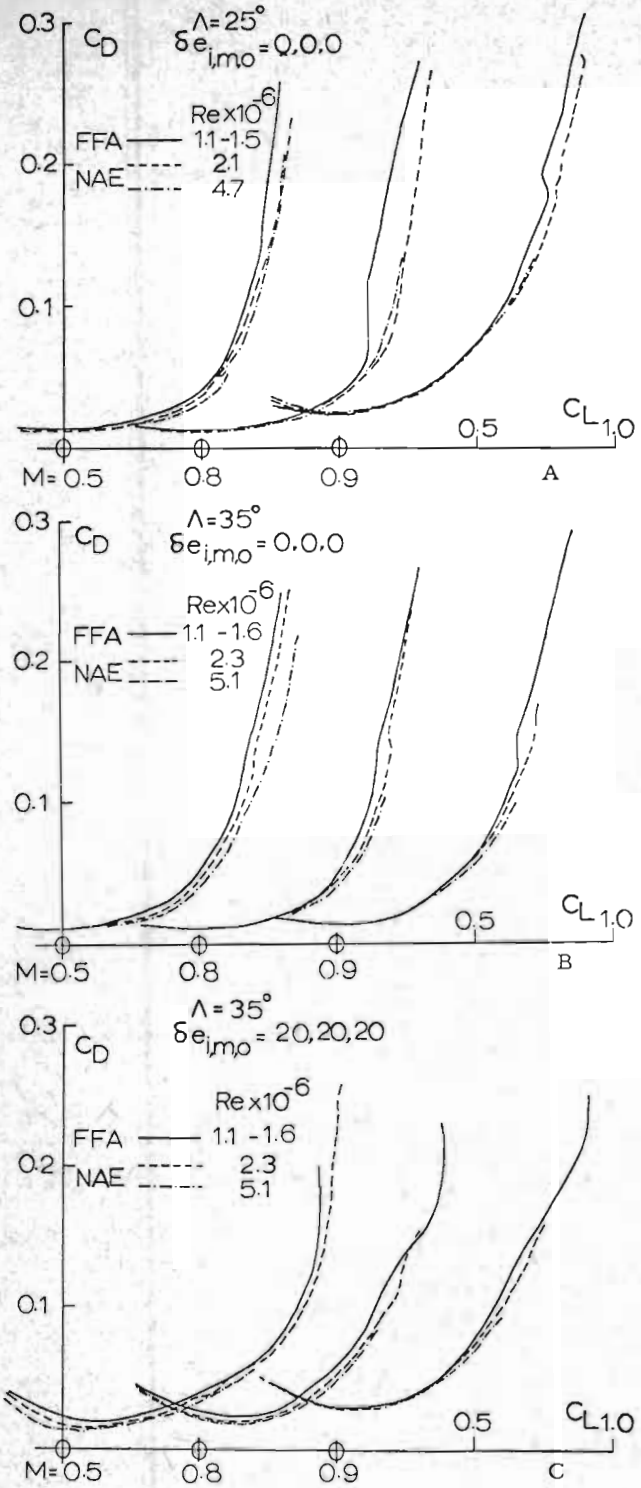

FIGURE 9 - COMPARISONS OF C_D VERSUS C_L AT THE VARIOUS MACH NUMBERS AND SWEEP ANGLES INVESTIGATED

In Figure 9 comparisons are shown of plots of the drag coefficient C_D versus the lift coefficient C_L at the low and high Reynolds numbers investigated. From this figure we see that the lift is increased for constant drag or the drag decreased for constant lift with increasing Reynolds number. This effect is largest for the models with sweep-back angles of 25° and 35°. For the configurations with drooped leading edge the gain in lift is smaller than for those with zero droop angle. See Figures 9B and 9C.

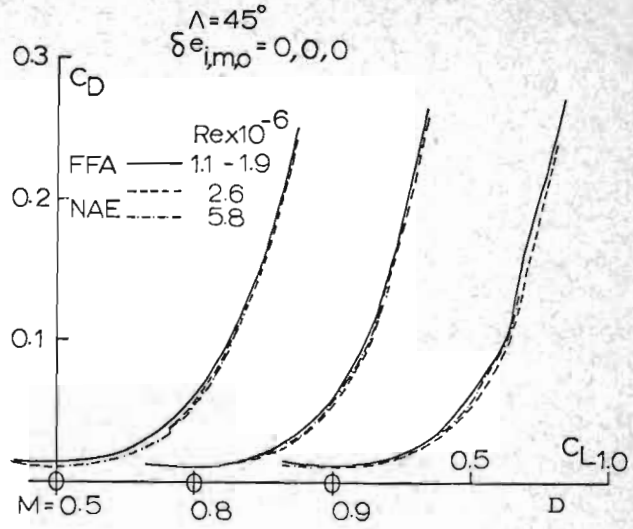

5.4 Reynolds Number Effects on Buffet Onset

The results of the wing root bending moment measurements performed on the 35° swept-back wing at M=0.5 and 0.9 in the FFA's S4 wind tunnel are presented in Figure 10. In this figure the RMS value of the root bending moment and the axial force coefficient are plotted versus angle of attack for the basic and 'drooped' configurations.

The RMS value of the bending moment is essentially invariant with angle of attack until some well defined break takes place. This point is indicative of buffet onset. For the basic configuration at both Mach numbers the measurements indicate reasonable correlation between the onset of buffeting and divergence in the static axial force. For the 'drooped' configuration, however, the correlation is good at the lower Mach number only. See Reference 6 where this type of correlation was extensively tested.

From Figure 8 we can see that the angle of attack for buffet onset increases with increasing Reynolds number for all configurations investigated. However, the improvement is smaller for the configurations with drooped leading edge flaps. As an example, the angle of attack for buffet onset plotted against Reynolds number is shown in Figure 11 for the 25° swept

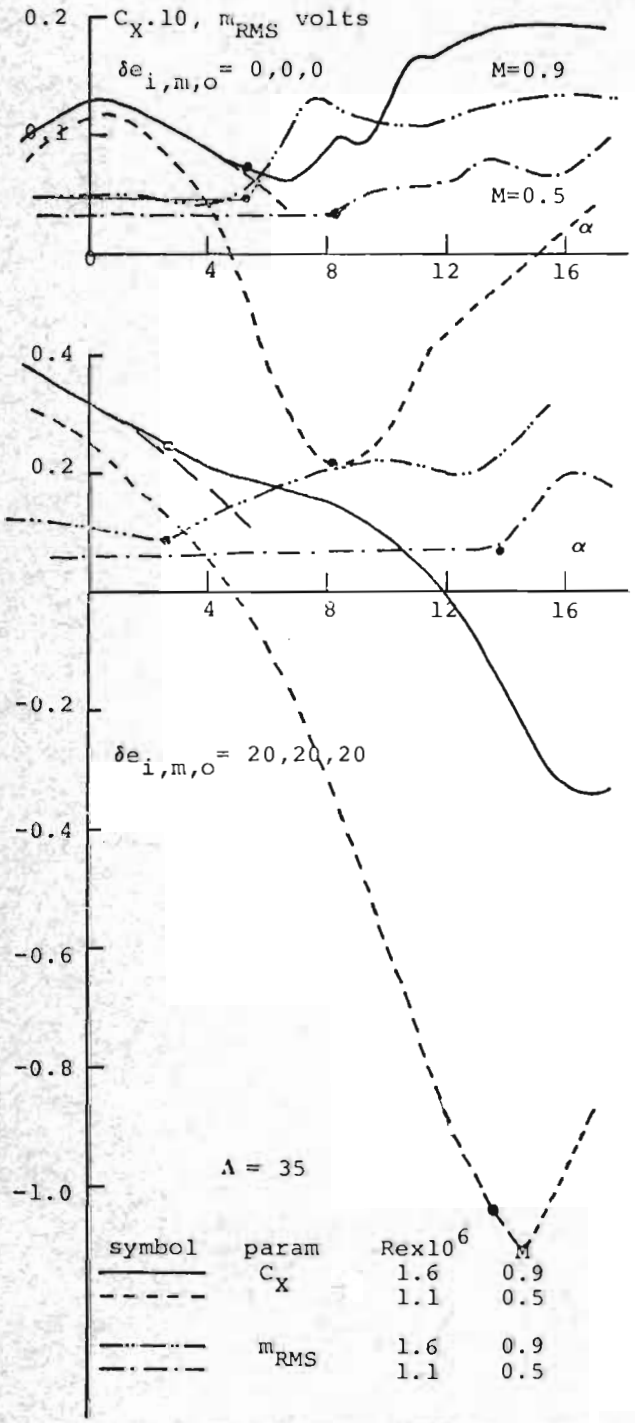

FIGURE 10 - C_X AND m_{RMS} VERSUS α CURVES AT M=0.5 AND 0.9 AT TWO DIFFERENT FLAP DEFLECTIONS

back wing at M = 0.5. The curve shows that the Reynolds number effect is progressive in the whole Re-range investigated. The continuous increase with Reynolds number in the angle of attack at which buffet onset occurs is the result of delayed separation with rising Reynolds number and thus related to the earlier discussed decrease in axial force.

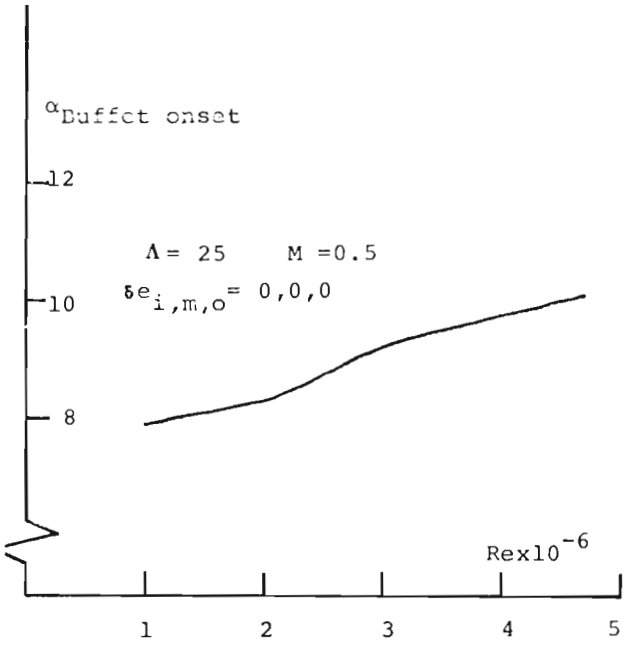

FIGURE 11 - ILLUSTRATION OF THE VARIATION OF ANGLE OF ATTACK AT BUFFET ONSET WITH REYNOLDS NUMBER

6. Effects of Leading Edge Sweep-Back

In Figures 12, 13 and 14 comparisons of the coefficients C_N, C_m and C_X versus α between the three sweep angles investigated are shown at the three Reynolds numbers used in the earlier figures. These are essentially cross plots of curves from Figures 5, 6

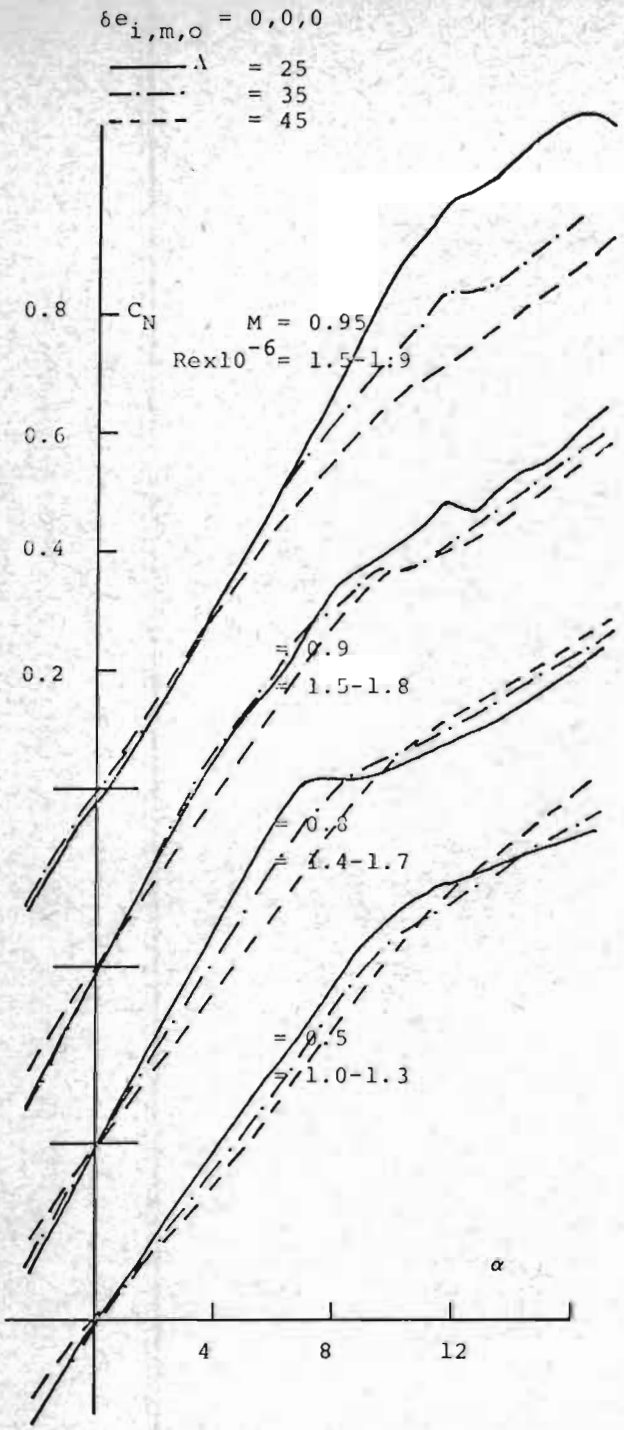

FIGURE 12A

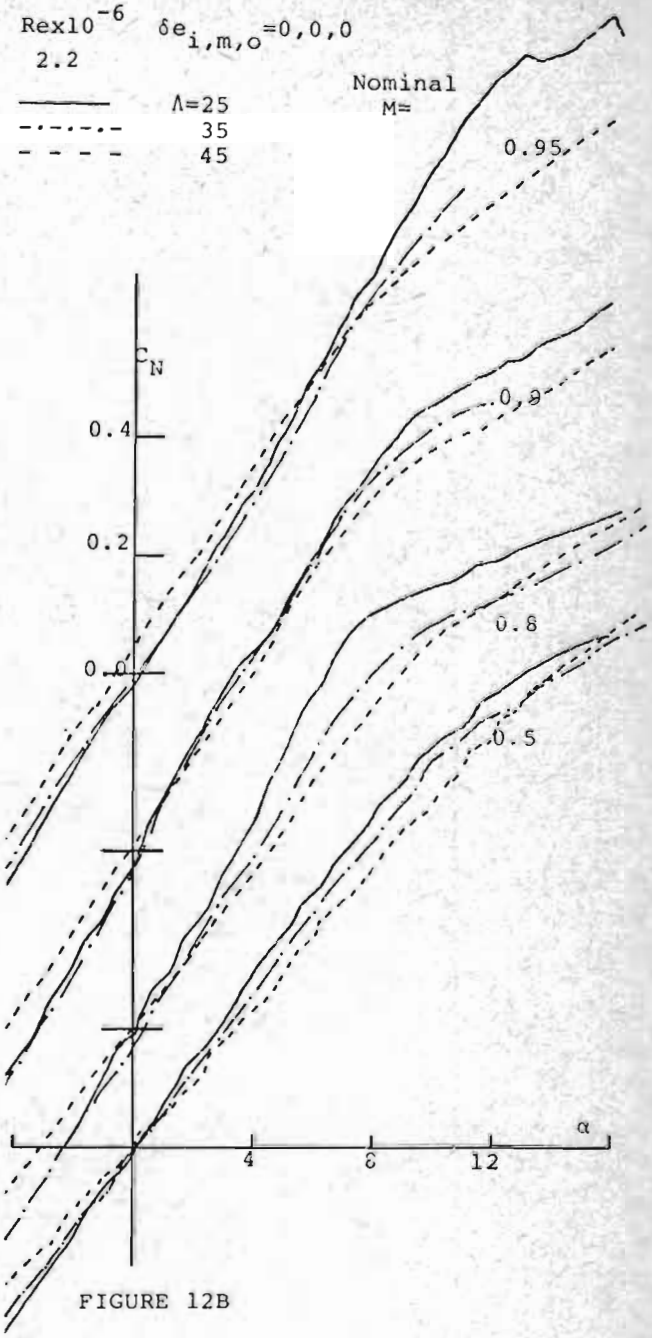

FIGURE 12B

FIGURE 12 - COMPARISONS OF C_N VERSUS α CURVES BETWEEN THE THREE SWEEP ANGLES INVESTIGATED AT THE VARIOUS TEST MACH NUMBERS

and 7. From Figure 12 it is seen that at the lower Mach numbers the normal force curve slope for small α decreases with increasing sweep angle as expected. At higher angles of attack the 25° swept wing stalls while the more highly swept wings produce a higher normal force partly due to vortex flow starting at the wing root as found for the 45° swept-back wing from flow visualization tests performed at FFA. At the higher Mach

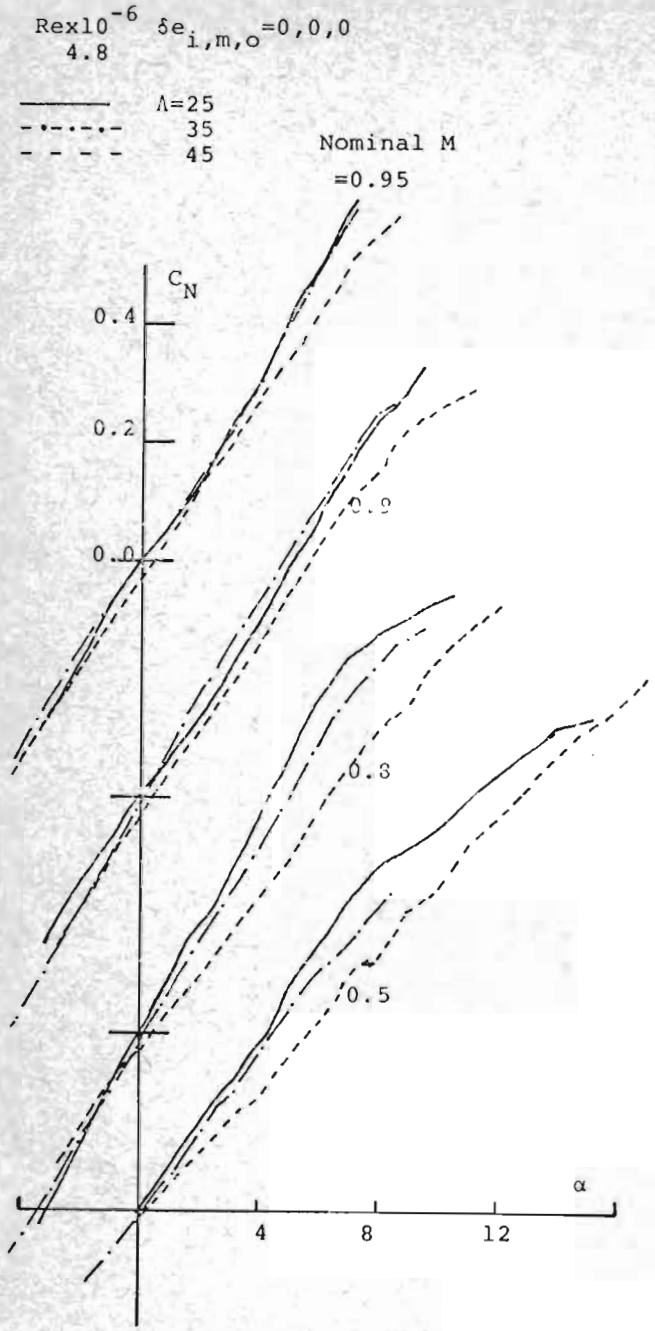

FIGURE 12C

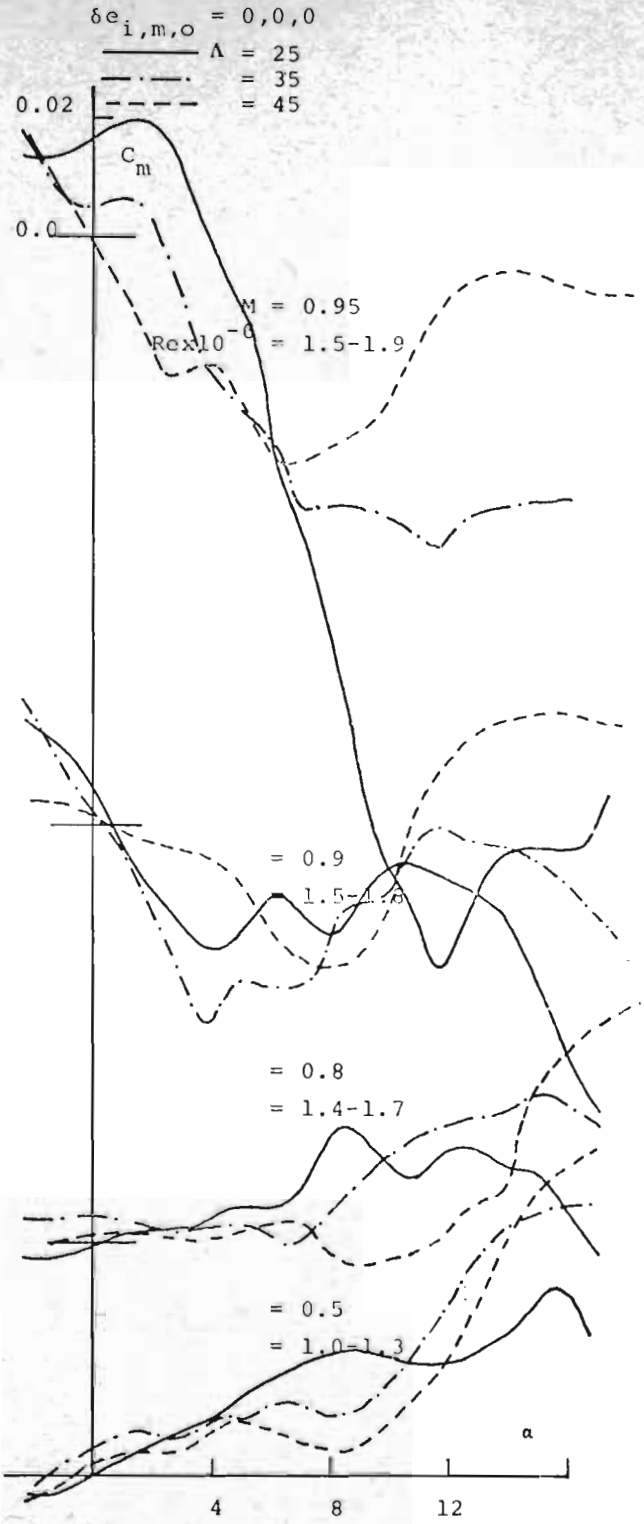

FIGURE 13A

FIGURE 13 - COMPARISONS OF C_m VERSUS α CURVES BETWEEN THE THREE SWEEP ANGLES INVESTIGATED AT THE VARIOUS TEST MACH NUMBERS

numbers the sweep-back effect is not so well defined; at M=0.95, for instance, the three wings have basically the same normal force curve slope at small α.

With regard to the pitching moment it is observed from Figure 13 that at higher Mach numbers the tendency for the pitch up condition occurs earlier, i.e. at a lower angle of attack, with increasing sweep-back, perhaps as a

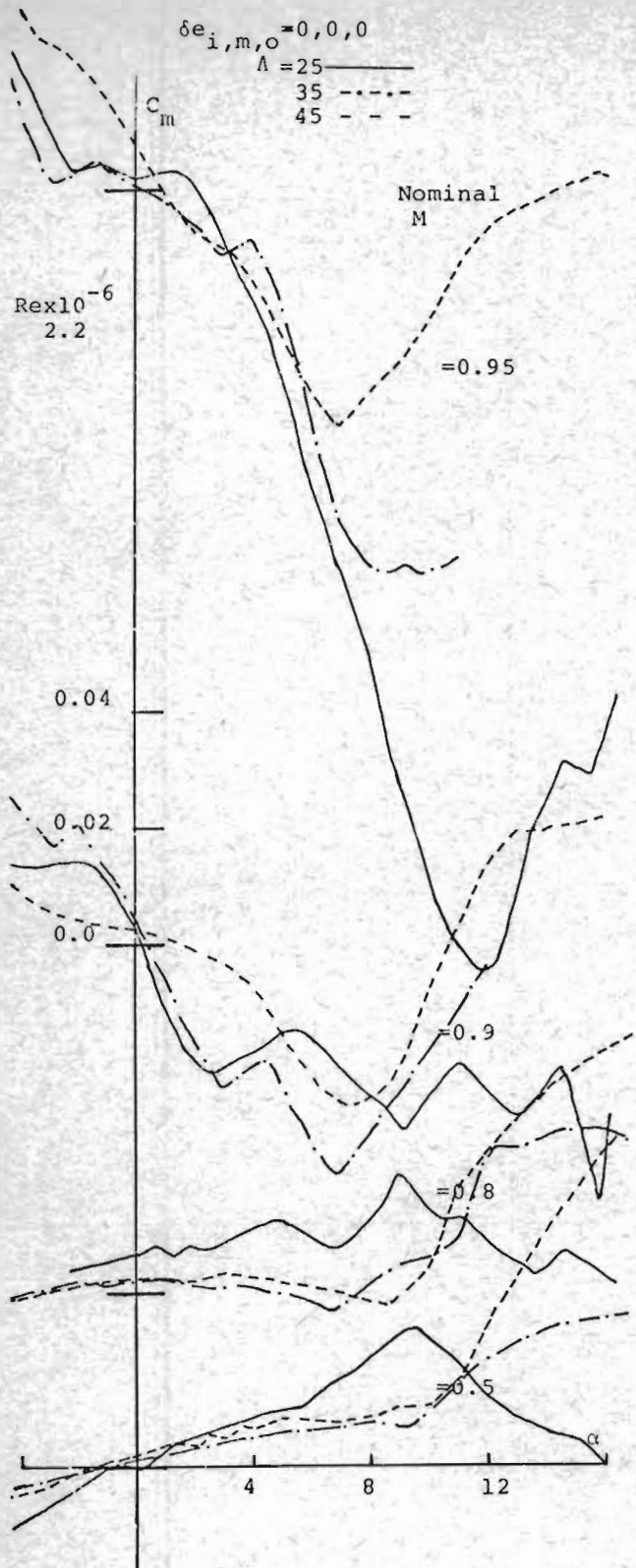

FIGURE 13B

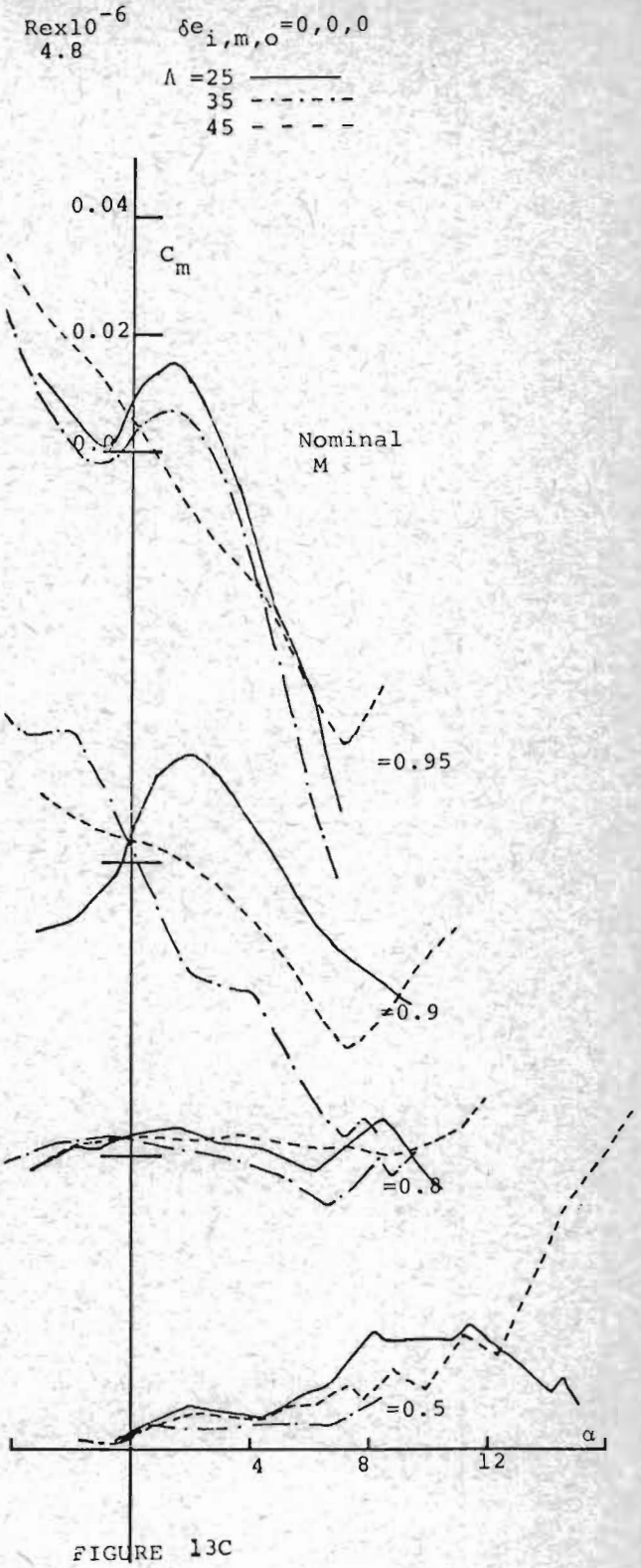

FIGURE 13C

result of tip stall because of the thickening of the boundary layer in this region. It is also seen that at high Mach numbers a reversed slope of the pitching moment curve occurs at small angles of attack for the 25° and 35° swept back wings but not for the 45° swept wing.

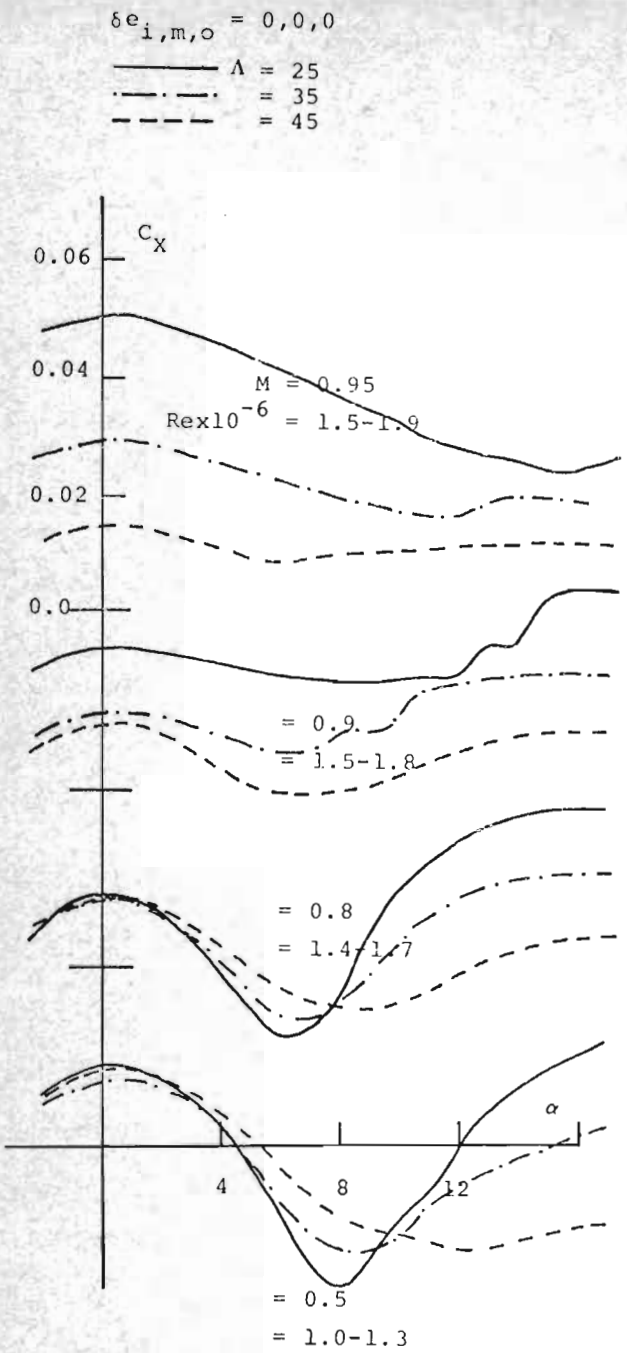

FIGURE 14A

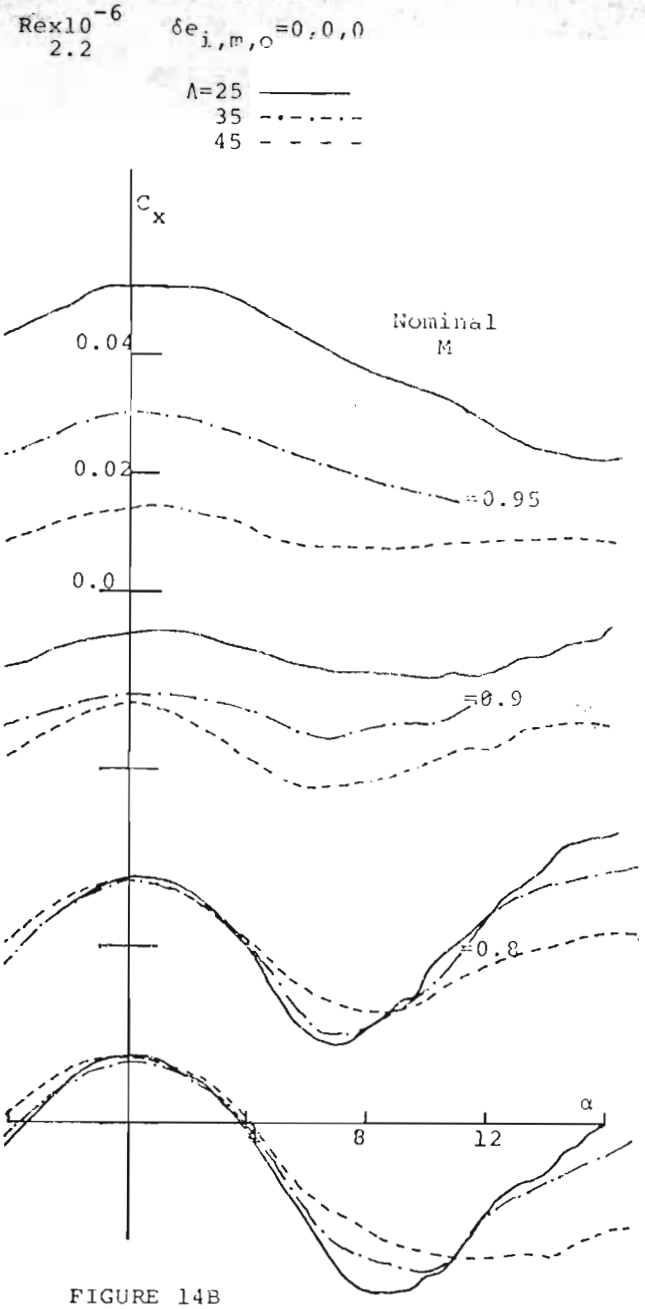

FIGURE 14B

FIGURE 14 - COMPARISONS OF C_X VERSUS α CURVES BETWEEN THE THREE SWEEP ANGLES INVESTIGATED AT THE VARIOUS TEST MACH NUMBERS

From the axial force curves shown in Figure 14 it is clear that the onset of separation occurs earlier on the 45° swept wing than on the lesser swept-back configurations. In particular at M = 0.5 where the axial force curves for the 35° and 45° swept-back wings show progressively earlier departure from that for the 25° swept-back wing.

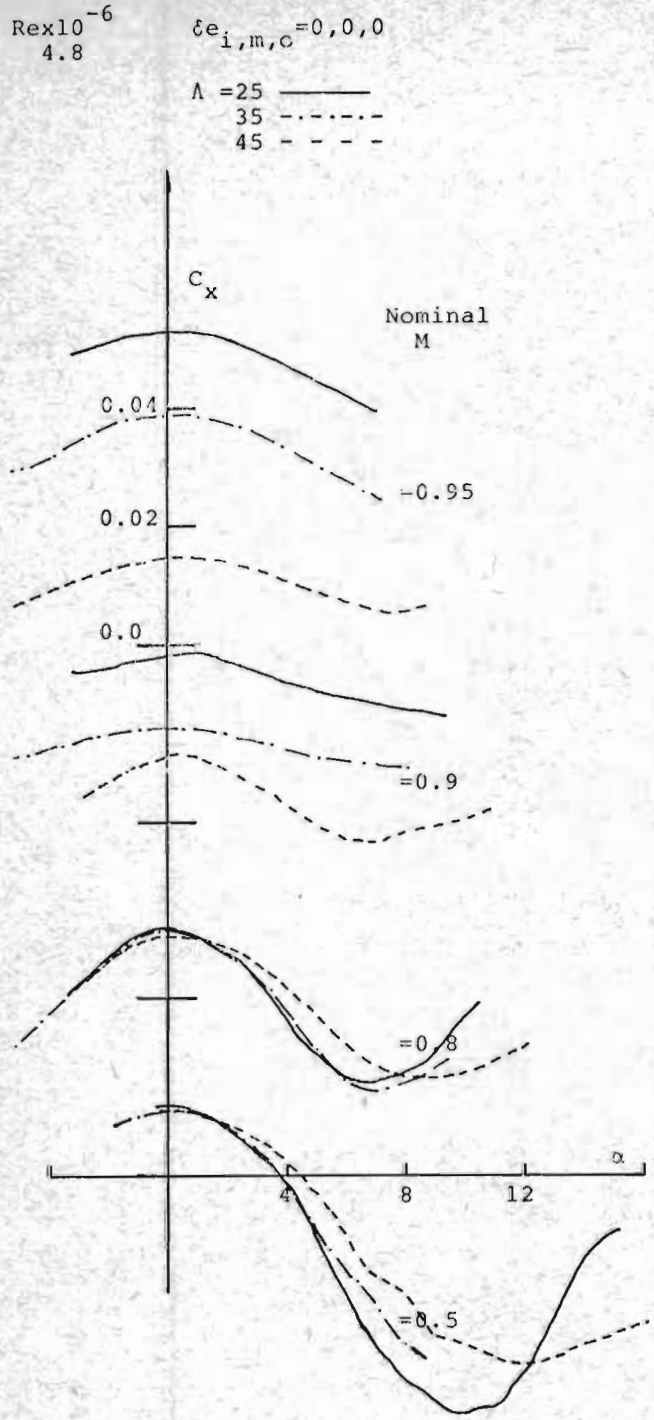

FIGURE 14C

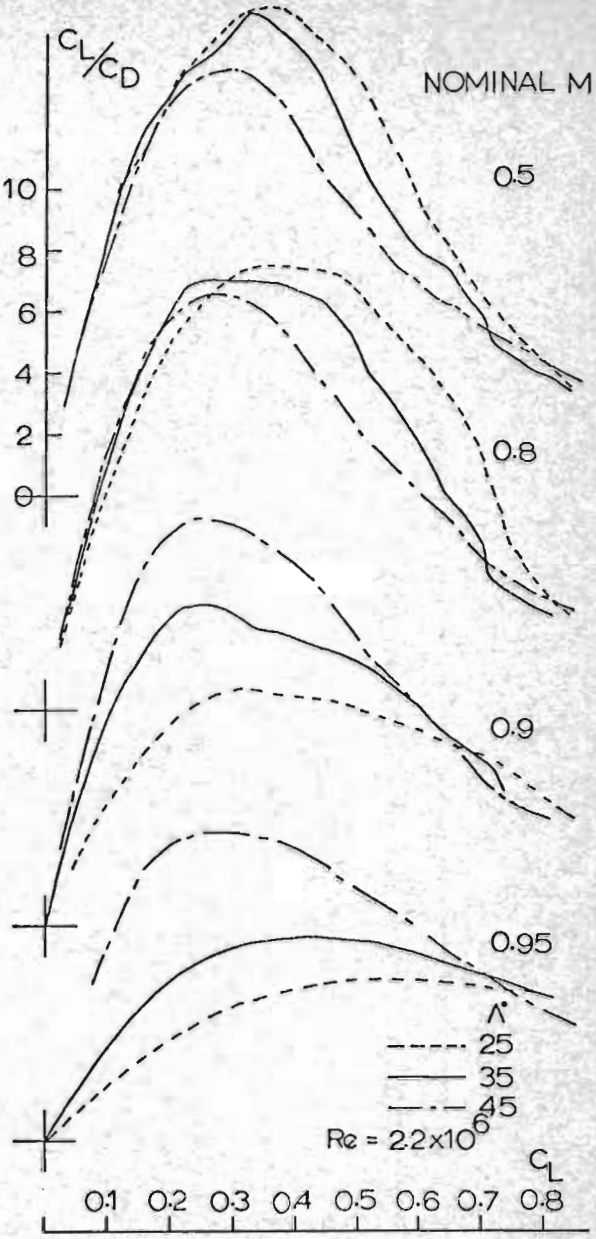

FIGURE 15A

FIGURE 15 - COMPARISONS OF C_L/C_D VERSUS α CURVES BETWEEN THE THREE SWEEP ANGLES INVESTIGATED AT THE VARIOUS TEST MACH NUMBERS

In order to assess the relative merits of the various sweep-back angles from the point of view of aircraft design a plot of the ratio C_L/C_D versus C_L has been prepared, see Figure 15.

From this figure the importance of sweep above the critical Mach number is easily appreciated at least at moderate C_L values. At high C_L values sweeping the

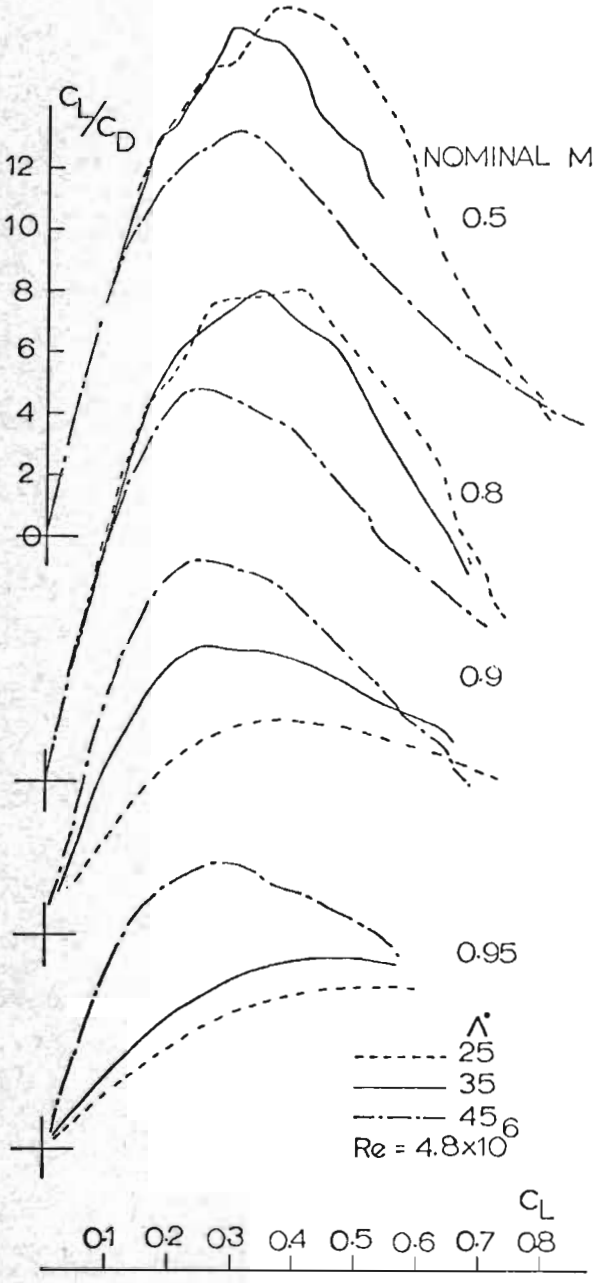

FIGURE 15B

wing has little effect over the magnitude of C_L/C_D. The general conclusions drawn are much the same at the two extreme Reynolds numbers examined at the NAE.

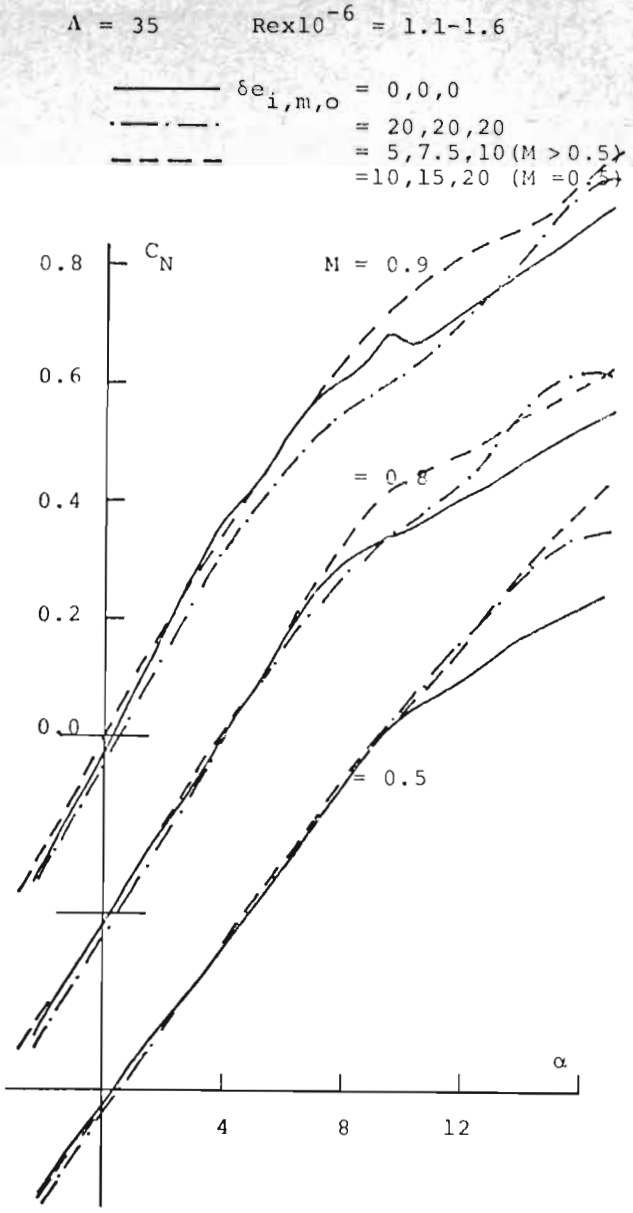

FIGURE 16A

FIGURE 16 - COMPARISONS OF C_N VERSUS α CURVES BETWEEN THE THREE TYPES OF LEADING EDGE DROOP INVESTIGATED AT THE VARIOUS TEST MACH NUMBERS

7. Effects of Leading Edge Droop

Comparisons of C_N, C_m and C_X versus α curves at the 35° sweep-back angle between the three types of leading edge droop investigated, namely, no droop, uniform droop of 20° and a variable droop along the span, demonstrate considerable and rather varied effects of both Reynolds and Mach numbers. See Figures 16,17 and 18. Because of the different ranges of angle of attack investigated in the various runs, in order not to exceed the capacities of the balance, it is difficult to draw specific conclusions. However, some of the most striking features are:-

Λ = 35 Re=2.2x10^6

——— $\delta e_{i,m,o}$=0,0,0
-·-·-·- =20,20,20
- - - - =5,7,5,10(M>0.5)
=10,15,20(M=0.5)

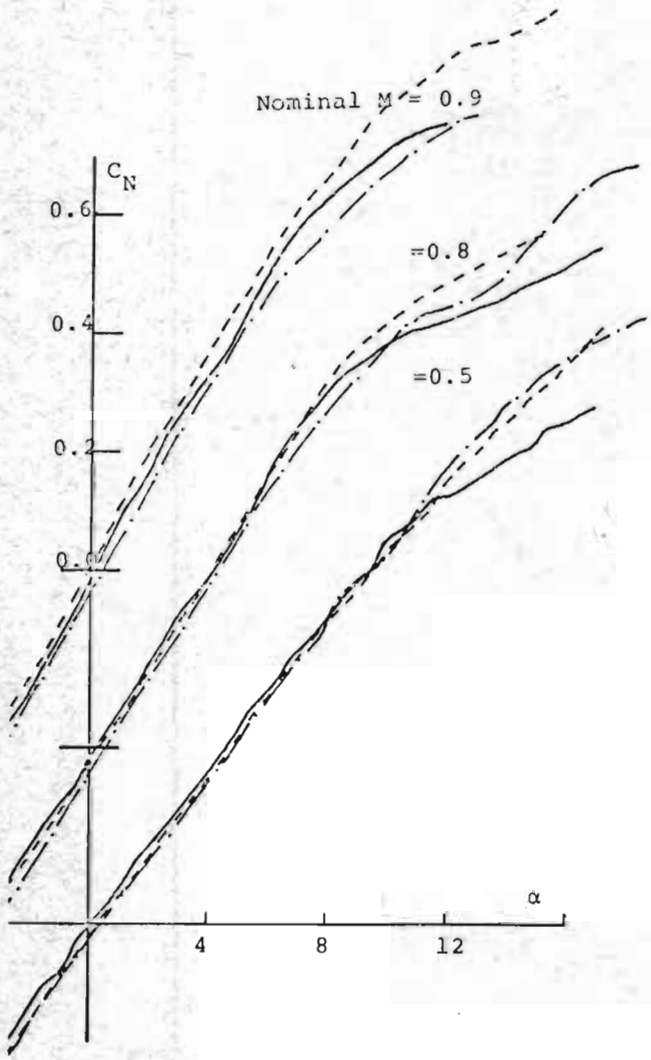

FIGURE 16B

Λ = 35 Re=4.8x10^6

——— $\delta e_{i,m,o}$=0,0,0
-·-·-·- =20,20,20
- - - - =5,7.5,10(M>0.5)
=10,15,20(M=0.5)

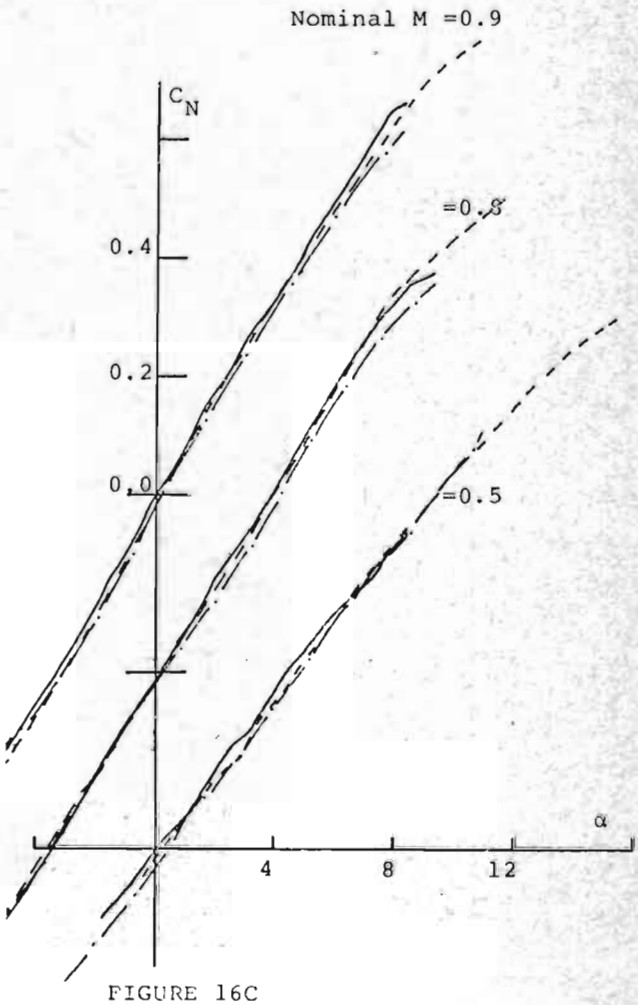

FIGURE 16C

a) The variable drooped leading edge configuration increases the normal force at high angles of attack compared with the basic wing for all Mach numbers and Reynolds numbers investigated. The uniform droop shows similar gains at Mach 0.5. At the higher Mach numbers the latter configuration has a lower normal force than the basic wing for intermediate angles of attack. At high Reynolds number the effect on normal force of both types of drooped leading edge is less pronounced than at the low Reynolds number.

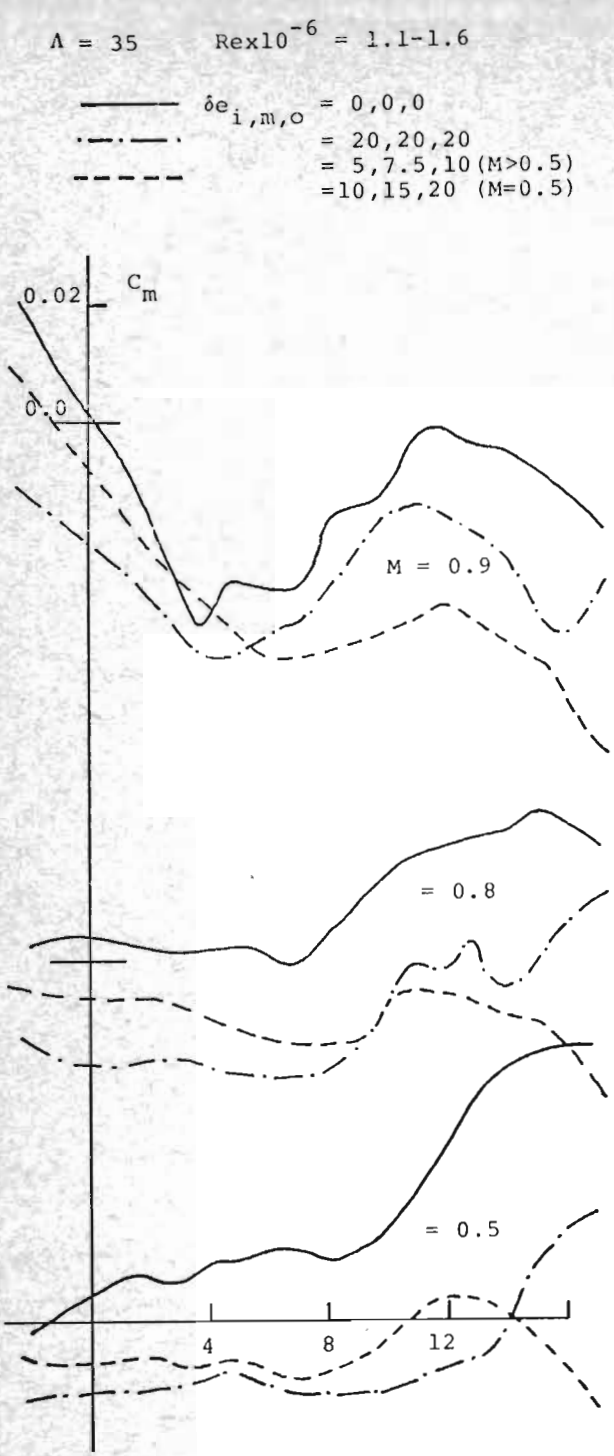

FIGURE 17A

FIGURE 17 - COMPARISONS OF C_m VERSUS α CURVES BETWEEN THE THREE TYPES OF LEADING EDGE DROOP INVESTIGATED AT THE VARIOUS TEST MACH NUMBERS

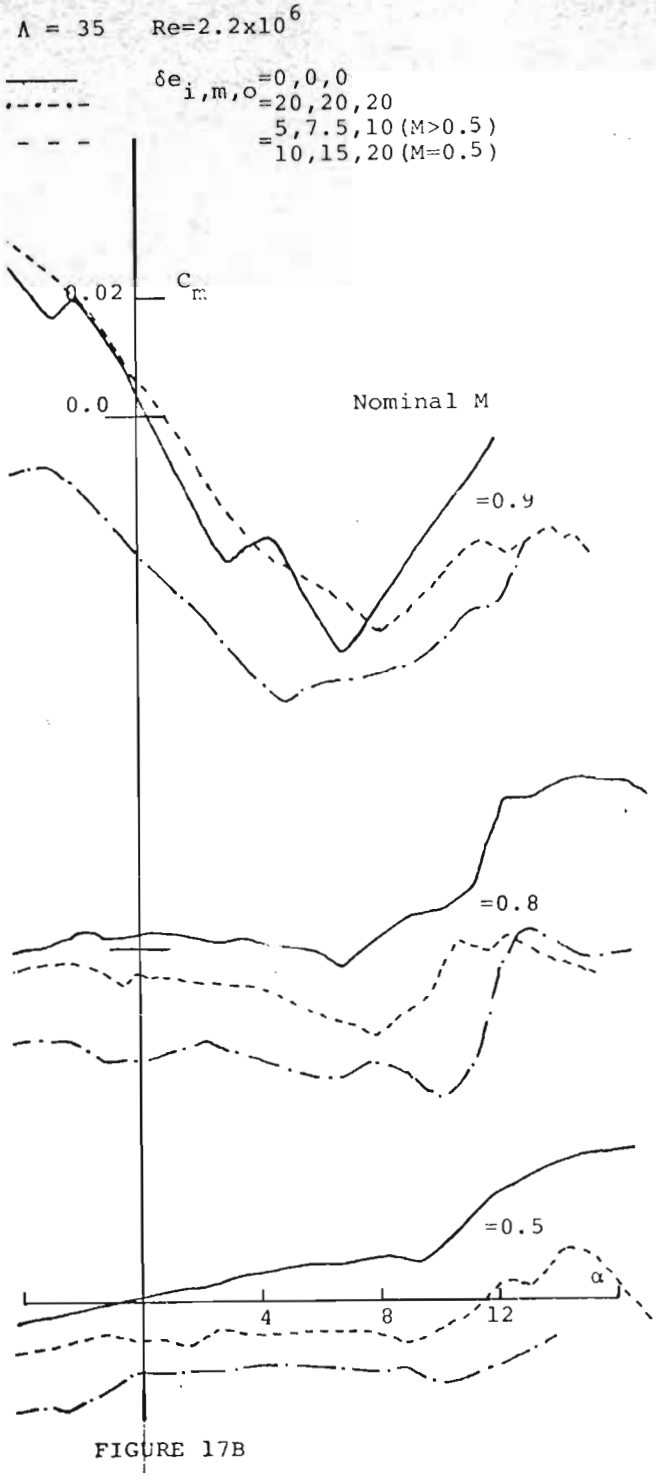

FIGURE 17B

b) drooping the leading edge produces a uniform decrease in the pitching moment as compared with that of the basic configuration. However, the variable droop produces a smaller shift than the uniform droop. This statement is true at all the Reynolds numbers investigated.

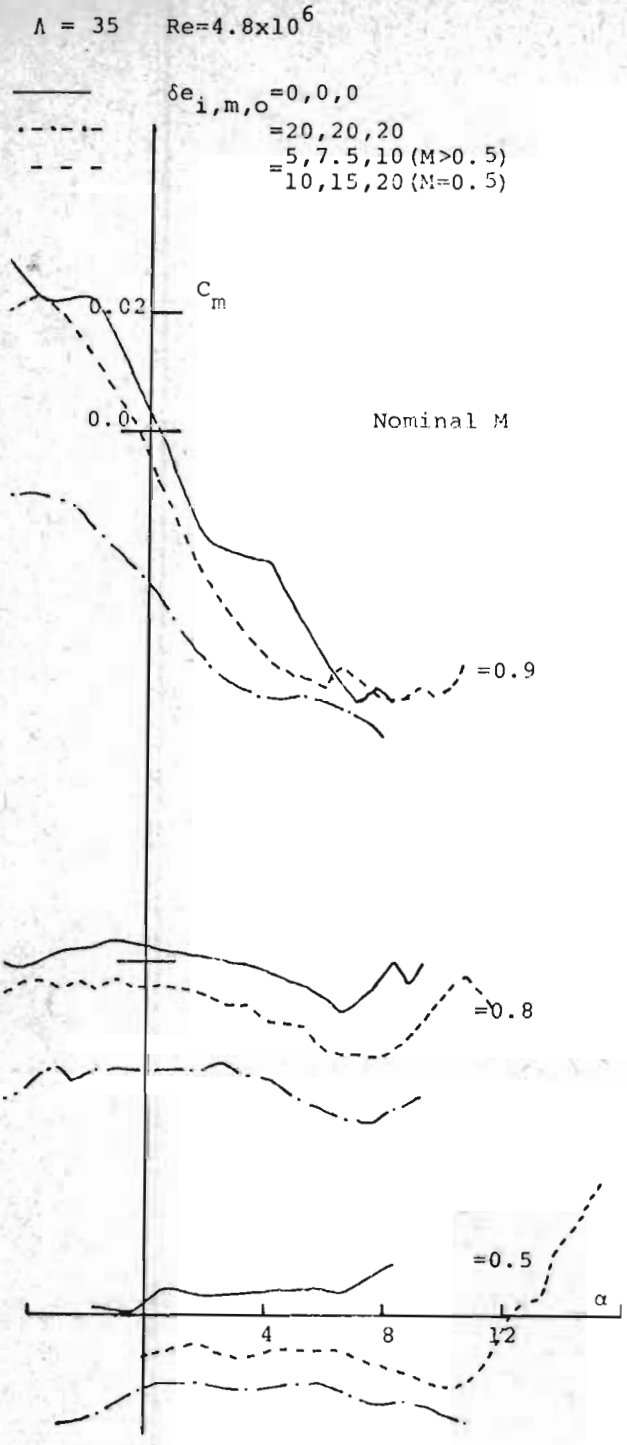

FIGURE 17C

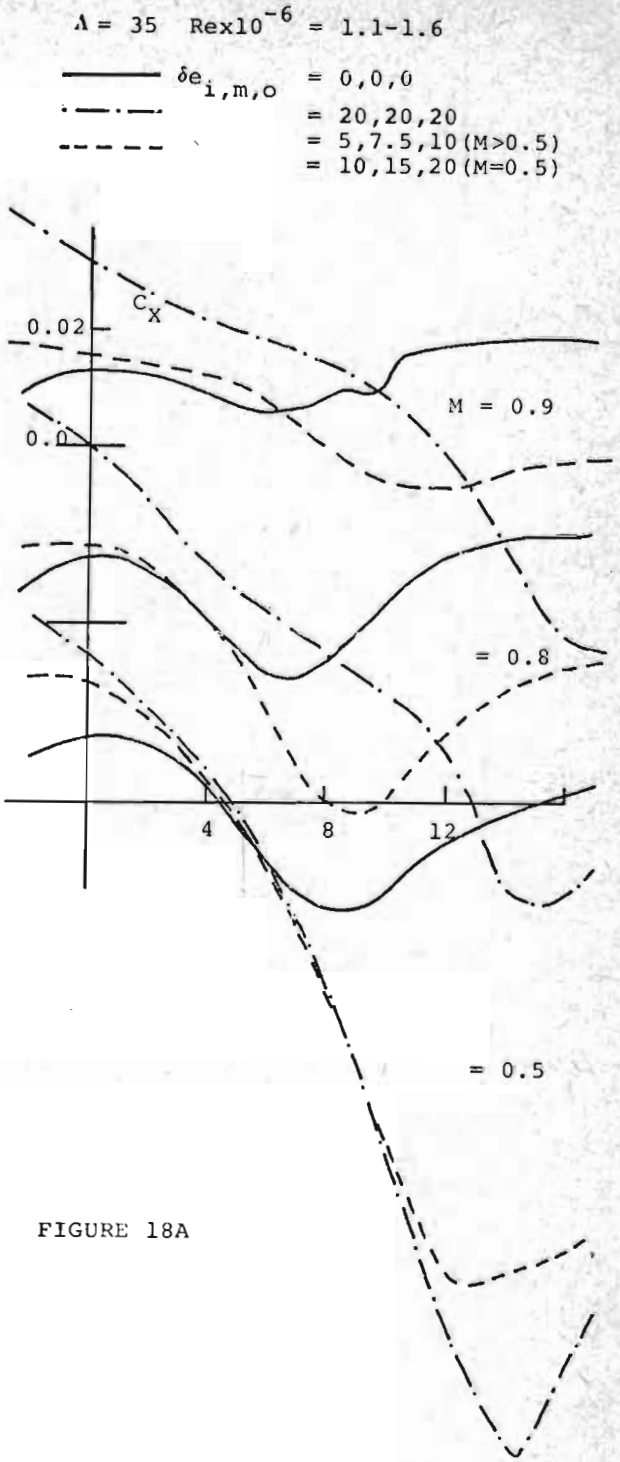

FIGURE 18A

FIGURE 18 - COMPARISONS OF C_X VERSUS α CURVES BETWEEN THE THREE TYPES OF LEADING EDGE DROOP INVESTIGATED AT THE VARIOUS TEST MACH NUMBERS

c) drooping the leading edge causes an increase in the axial force coefficient over that of the basic configuration at low angles of attack but a reduction of same at high angles. At the low Mach number tested M=0.5, the increase in C_X at low angles of attack due to drooping the leading edge is much reduced with increasing Reynolds number. However, the Reynolds number has virtually no effect on similar increases in C_X at higher Mach numbers. At moderately high angles of attack there is some reduction in C_X at all three Mach numbers tested. At each Mach number these decreases in C_X are of about the same magnitude at all Reynolds numbers investigated, i.e.

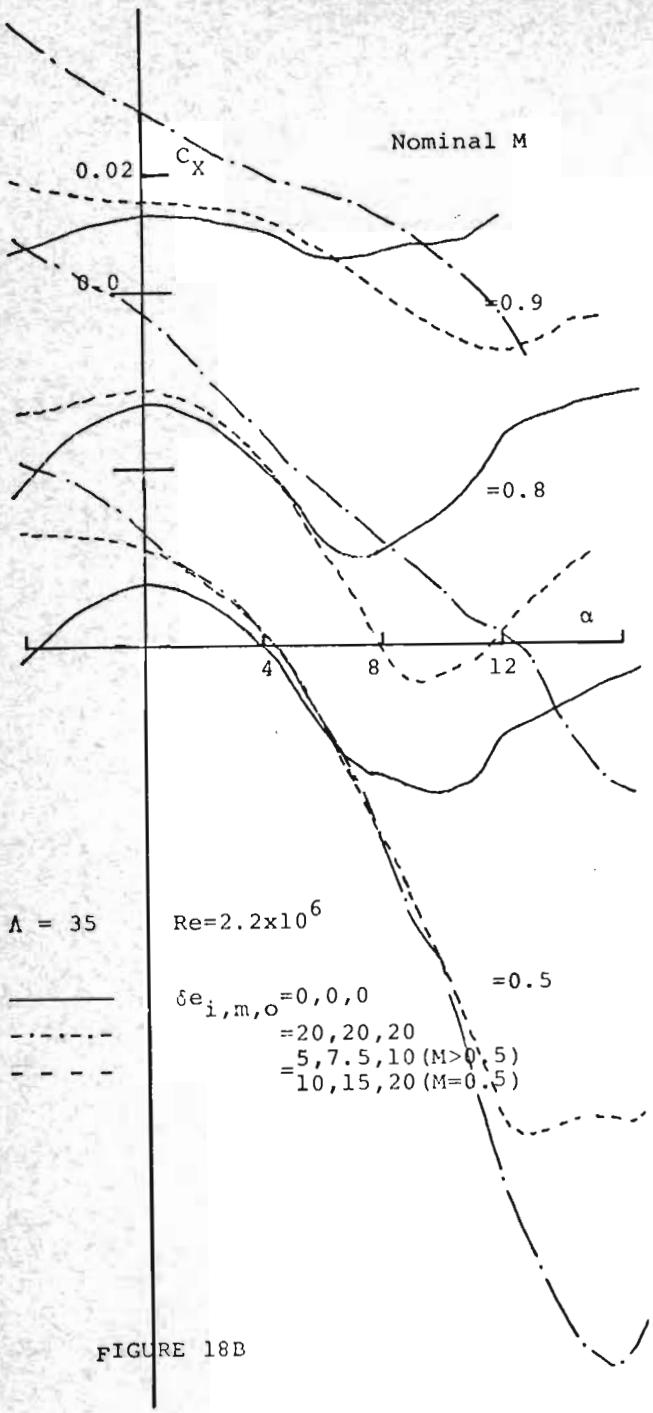

FIGURE 18B

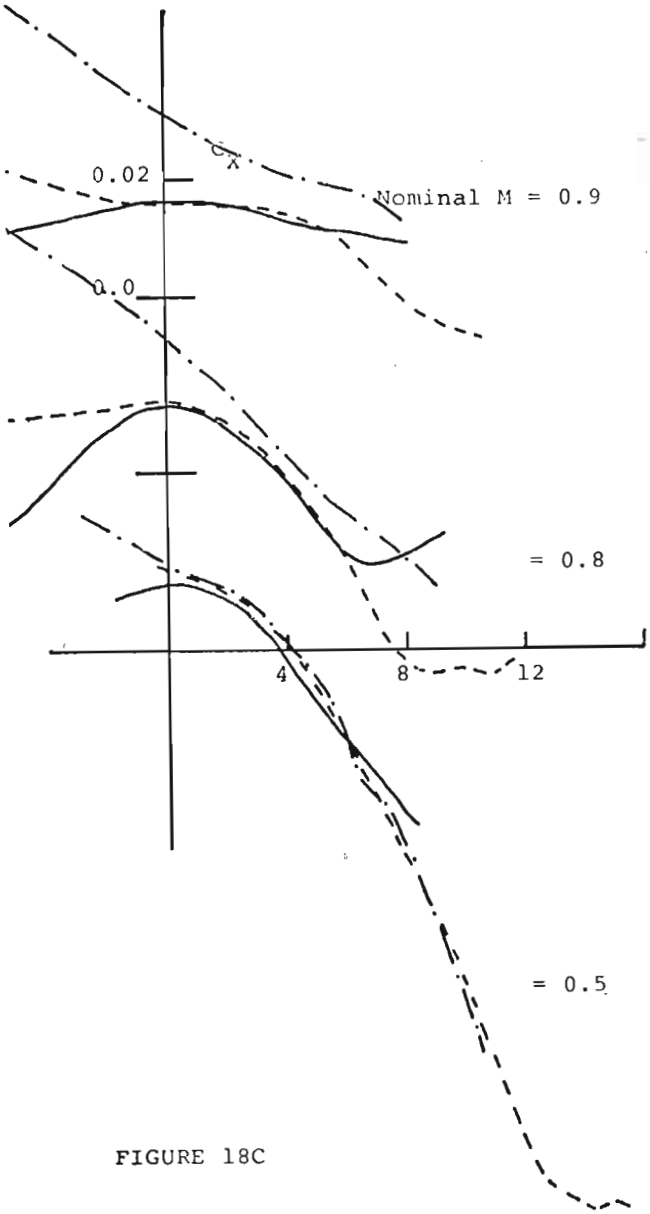

FIGURE 18C

independent of Reynolds number. The variable droop of 5°, 7.5° and 10° shows a larger decrease in C_X at M = 0.8 and 0.9 over the uniform droop of 20° up to the maximum Reynolds number of the present investigation. At still higher angles of attack the uniform droop of 20° shows a tendency towards achieving greater reductions in the axial force coefficient at all Mach numbers and up to the highest Reynolds number investigated.

From Figure 18B it can also be seen that at Mach number 0.5 the angle of attack for buffet onset is increased with drooping the leading edge. For this Mach number and low Reynolds number the angle of attack at buffet onset increases from 8° for the basic model to 12° for the configuration with variable droop and to a still higher 14° for the configuration with uniform droop.

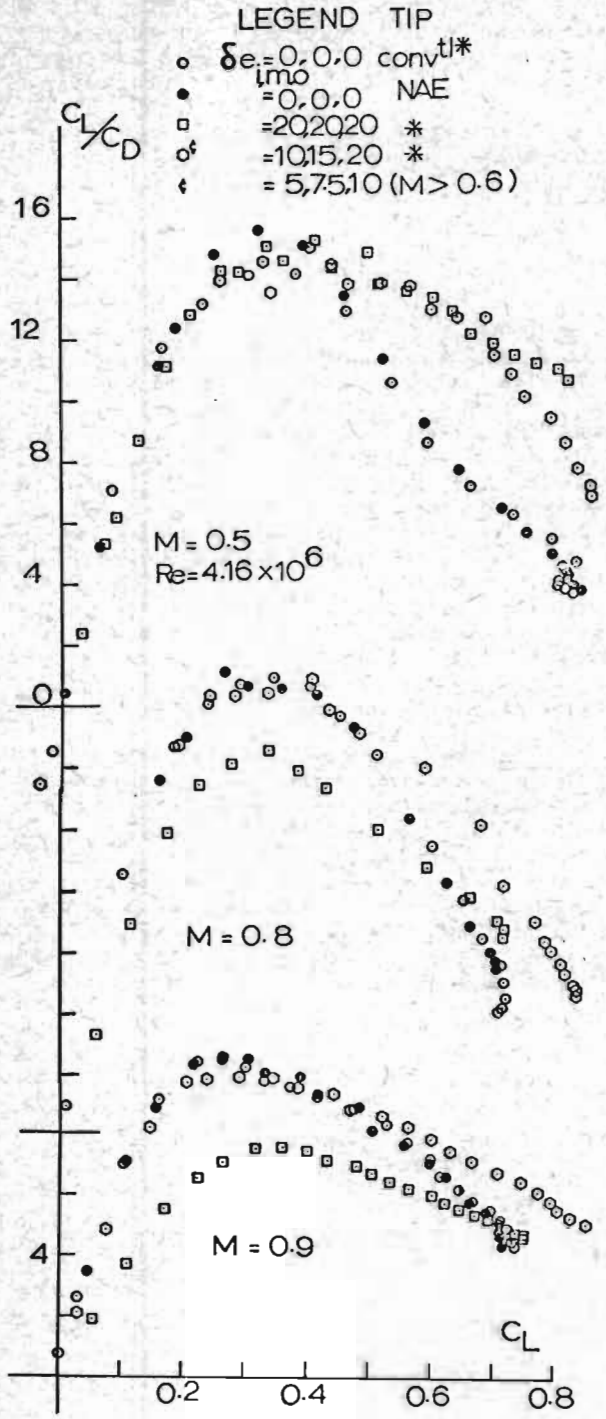

FIGURE 19 - COMPARISONS OF C_L/C_D VERSUS α CURVES BETWEEN THE THREE TYPES OF LEADING EDGE DROOP INVESTIGATED

To illustrate more clearly the benefits of the different types of leading edge droop we have provided plots of the ratio C_L/C_D versus C_L in Figure 19. An intermediate Reynolds number was chosen at which the NAE proposed tips were tested so that a comparison between the straight and the NAE proposed wing tips can be made. We see then from this figure that at M = 0.5 the variable droop of 10°, 15°, 20° is not as effective as the 20° uniform droop. However, both types of droop show improvement in performance over that of the basic wing especially at the high angles of attack. At the two higher Mach numbers examined, namely, 0.8 and 0.9, the uniform 20° droop is much too high causing a deterioration of the wing performance as compared with the basic wing. On the other hand the variable droop of 5°, 7.5° and 10° maintains more or less the performance of the basic wing at low and moderate C_L values and shows improvement over the basic wing at higher C_L values.

It is further observed that the NAE proposed type of wing tips show some definite improvement over the straight tips at Mach 0.5 with increasing Reynolds number, providing a 10% improvement in the maximum C_L/C_D. At higher Mach numbers this improvement in (C_L/C_D) max is not realised.

8. Conclusions

Reynolds number effects in the range $1\times10^6 < Re < 5\times10^6$ and $0.5 < M < 0.95$ were investigated experimentally on swept-wing-body configurations with various degrees of leading edge droop and with straight and upwardly curved wing tips. The following conclusions are reached:-

1) generally the benefits achieved at low Reynolds number through the use of leading edge droop are not realised to the same degree at high Reynolds number

2) at supercritical Mach numbers, M=0.9 and 0.95 for the 25° swept wing and M=0.95 for the 35° swept wing, the pitching moment coefficient at low angles of attack shows a noticeable Reynolds number dependency resulting in a reversed sign of the C_m versus α curve as the Reynolds number is increased

3) at high angles of attack at M=0.5 the effects of an increase in the Reynolds number on the axial force coefficient of all configurations is to progressively decrease C_X. This decrease shows no sign of tapering off towards the highest test Reynolds number

4) the benefit of increasing sweep-back is to delay the drag rise to a higher Mach number and to provide a higher normal force at high angles of attack. Its disadvantages are to reduce the normal force curve slope at low Mach numbers and to suffer from buffeting at lower angles of attack

5) beneficial effects are observed through the use of upwardly curved wing tips at M=0.5 with increasing Reynolds number. At Re=4.16x10⁶ the upwardly curved tips provide a 10% improvement in the maximum C_L/C_D achieved by using the straight wing tips.

9. References

1. Hancock, G.J., Role of Fluid Dynamics in Aircraft Stall and Post Stall Gyrations.
AGARD, Conference preprint 102, paper 1, April 1972.

2. Sorensen, H., Undersokning av schematiska FPL-konfigurationer.
Sexkomponentvagningar och stromnings-undersokningar pa fpl-modell med 50° pilvinge och nosklaff.
FFA Provbesked AU-724-P1 och P2.
December 1970, Januari 1971.
(Investigation on Schematical Aircraft with swept wings.
Six component balance tests and oil flow tests on swept Wing Body configurations with a sweep-back angle of 50° and leading edge flaps.)

3. Thain, J.A., Reynolds Number Effects at Low Speeds on the Maximum Lift of Two Dimensional Aerofoil Sections Equipped with Mechanical High Lift Devices.
Reprint DME/NAE Quarterly Bulletin No.1, 1973 (3), National Aeronautical Establishment, Canada.

4. Moss, G.F., Haines, A.B. and Jordan, R., The Effect of Leading Edge Geometry on High Speed Stalling.
AGARD, Conference preprint 102, paper 13, April 1972.

5. Foster, D.N., The Low Speed Stalling of Wings with High Lift Devices.
AGARD, Conference preprint 102, paper 11, April 1972.

6. Edward, J. Ray and Taylor, R.T., Buffet and Static Aerodynamic Characteristics of a Systematic Series of Wings Determined from a Subsonic Wind-Tunnel Study.
NASA Technical Note, NASA TN D5805, June 1970.

7. Atraghji, E., Effects of Reynolds Number on Swept Wing Body Configurations with High Lift Devices in Transonic Flow.
Project Report 5x5/0066 to be published.

8. Sorensen, H., Effects of Reynolds Number on Swept Wing Body Configurations with leading Edge Flaps in Transonic Flow.
FFA Technical Note AU 934 - to be published.

DISCUSSION

A. Das (DFVLR, Braunschweig, Germany): Your paper presents a detailed experimental analysis of the flow behaviour of swept wings in a wide range of angle of attack, wing-sweep and Reynolds number. From these a general conclusion has been drawn also for the flow conditions at large angle of attack whereby at the wing tips complicated flow phenomena comes into play, namely separation, rolling up of vortices, vortex bursting etc. which are influenced by the particular wing geometry. So a correlation of the various results in the region of high angle of attack is difficult - the conclusions drawn out from these results may then have limited validity. Investigations with some more wing geometries may give more insight and confirm the general conclusions drawn in this paper.

E. Atraghji and H. Sorensen: Our test was restricted to angles of attack below the stall boundary but well within the region of buffet onset. Achieved angles of attack reached 16° in some cases but even then no large scale separation of the flow occurred. The conclusions reached in the paper apply only to pre-stall conditions. No doubt further tests conducted with different wing geometries could provide some further insight and hopefully substantiate the general conclusions drawn in our paper.